

**MINISTRY OF EDUCATION
AND TRAINING**

**MINISTRY OF INDUSTRY AND
TRADE**

**NATIONAL RESEARCH INSTITUTE
OF MECHANICAL ENGINEERING**

Ph.D CANDIDATE: NGUYEN MINH TAN

**A STUDY ON RESISTANCE SEAM WELDING TECHNOLOGY
FOR RESTORING SHAFT PARTS**

SPECIALIZATION: MECHANICAL ENGINEERING

CODE No: 9520103

SUMMARY OF ENGINEERING Ph.D THESIS

HA NOI – 2019

**Training institutions: National Research Institute
of Mechanical Engineering –Ministry of Industry and Trade**

Full name of the scientific supervisor:

- 1. Dr. Hoang Van Chau**
- 2. Assoc. Prof. Dao Quang Ke**

Reviewer 1:

Reviewer 2:

Reviewer 3:

**Proposal thesis was defended under scientific committee at National
Research Institute of Mechanical Engineering –Ministry of Industry and
Trade.**

Address: No.4 Phạm Van Dong - Cau Giay - Ha Noi

At ... am ..., date ... month ... year 2019

Reference at:

National library;

Library of National Research Institute of Mechanical Engineering;

Library of Hung Yen University of Technology and Education

INTRODUCTION

1. Rationale

In the process of State industrialization and modernization, accompanied with the integration and acquirement of science – technological advancement in the investment of modern equipment from advanced nations, it is important to create and promote inner forces and control technology. The application of research achievements in scientific and technical progress helps manufacture products that can meet the demands as the imported products do; however, it is essential that the price should be suitable with the capacity of manufacturing facilities.

In the field of welding technology, together with the application of advanced welding technology into manufacture to increase the quality and reduce the product price, it also becomes a concern of this technology application for reinstatement and enhancement of machine element quality, saying that it has been implemented effectively.

Over the past years, Vietnam has developed the industry through importing subassembly and separated equipment from many countries in the world. In order to ensure and maintain the effective long-term operation, reinstatement technology for used accessories plays an important role. Price for reinstatement of broken-down accessories is not in excess of 30 to 50% in comparison with the price of a new replacement. There are many complicated machine elements; however, with reinstatement accounting for 15 to 20% of their prices, they can operate with full functions and their quality is as good as the new ones.

For the increasing demand of science and technology, the thesis “**A Study on Resistance Seam Welding Technology for Restoring Shaft Parts**” focuses on addressing the technology implementation, mathematics equation construction which reflects the relationship between the quality of welded layer and the welding parameters. Design management and full development of welding procedure not only contributes significance in terms of economy but also the particular values in terms of science and technology. Additionally, it helps create a new research direction for welding-based reinstatement of axis-shaped machine parts, providing efficiency, quality, and economic effectiveness and typically protecting the natural resources and the environment in our country.

2. Research objective of the thesis

+ To systematize science basis, thereby experiment and apply resistance seam welding technology for restoring the shaft with filler steel wire on existing experimental equipment in Vietnam.

+ To enhance the effectiveness and quality of reinstatement of broken-down accessories based on the innovation of resistance seam welding procedure using the filler steel wire.

+ To develop mathematics equation which reflects the relationship amongst technological parameters including welding current intensity I_h (kA), electrode pressure force F (kN), welding speed V_h (cm/s) to fillet welding quality.

3. Object and Scope of study

+ *Object of study:*

- Resistance seam welding technology to recover shaft details with filler steel materials
- Study the quality of the cover metal layer on the surface of the C45 steel shaft by resistance seam welding technology with filler steel C70.

+ *Scope of study:*

- Quality of welding layer for reinstatement of surface steel shaft, which was made of C45 material and has a diameter of 50÷150mm by using resistance seam welding with filler wire C70. Conducting a quality assessment of the welded sample in terms of bonding strength between the welded metal and axial substrate metal, hardness and abrasion resistance, macrostructure, microstructure and chemical compositions of added metal. Based on the collected data, conducting analysis and assessment of technical parameters such as (assess the influence of technological parameters as) welding current intensity I_h , electrode pressure force F , welding speed V_h to the quality of fillet welding for reinstatement.

4. Methodology

Combination of empirical and theoretical study

+ *Theoretical study:*

- Study on operating principle, damaged forms of the shaft, especially the damage by abrasion.

- Analysis and generalization of welding technology for reinstatement of machine elements by resistance seam welding with filler steel wire, surveying relevant studies.

+ *Experimental study:*

- Study in the functional transformation of resistance seam welding, in combination with fixture device to implement the resistance seam welding technology for reinstatement of the axis-shaped machine details.

- Construction of experimental model based on analysis of inputs and output objections of the welding procedure; Calculation to identify the standard parameters and combinatory of experimental methods in accordance with the Taguchi method.

- Based on the results, checking the mechanical properties of fillet welded layer, using analysis of variance ANOVA and Multiple Regression with Many Predictor Variables to review the research results as the set-out goals.

- Reliability and effectiveness of the methods that will be checked through a verification experiment to serve as an applicable base for research results.

5. Scientific and practical significance of the thesis

5.1. Scientific significance

- By experiment, pointing out the relationship between 03 parameters of resistance seam welding: I_h , F , V_h with mechanical properties and microstructure of the welded area, thereby, assessing the welding forming mechanism and material structure near the welded regions.

- Proposals for a set of resistance seam welding parameters, pair of steel material C45 or 40Cr with the coating by steel wire C70 on the existing experimental equipment in Vietnam, ensuring the reinstatement quality of the shaft.

- Identification of the combination of 3 parameters: I_h , F , V_h , aiming at gaining the highest mechanical properties in the investigated area and quantify the effect ratio of these parameters on mechanical properties of the hardfacing layer.

5.2. Practical significance

- Thesis results can be the reference for welding technology field, serving for the application and manufacture research.

- Completing a restoration technology of the shaft machine elements which contributes certain effectiveness in terms of capacity, quality, economy, and protection of natural resources and the environment in our country.

- Construction of proper assessment methodology for the hardfacing layer by using resistance seam welding technology for shaft components with low abrasion.

6. New contribution of the thesis

- Broadening the application scale of resistance electric seam welding technology in the field of repairing and restoration of shaft for good productivity, quality, low costs, and environmental safety in our country.

- Identifying the role of influence of some technology parameters (I_h , F , V_h) toward the quality of reinstatement welding layer, serving as a scientific base for the other similar studies.

- Constructing the regressing equation that presents concurrent relationships of parameters I_h , F , V_h influencing mechanical properties of hardfacing layer on conducting resistance seam welding for restoring of shaft parts.

- Conducting Grey Relational Analysis (GRA) in combination with the Taguchi and Double division algorithm to find out the optimal value, the percentage of influenced technological parameters that simultaneously meet multiple objectives of mechanical properties of the welded joint

7. Dissertation Outline

Besides the Introduction and the Sections as per regulations, this paper consists of 04 chapters and the general conclusion of the thesis.

- Chapter 1. Overview of resistance seam welding technology for restoration of the shaft machine parts.

- Chapter 2. The theoretical foundation of resistance seam welding technology for restoration of the shaft machine parts.

- Chapter 3. Materials, equipments, experimental methods and evaluations

- Chapter 4. Experimental results and discussions

- The general conclusion of the thesis

- Reference, publication lists of the thesis, appendix thesis.

CHAPTER 1. OVERVIEW OF RESISTANCE SEAM WELDING TECHNOLOGY FOR RESTORATION OF SHAFT PARTS

1.1. Features and methods of restoration of shaft parts

1.1.1. Material for shaft manufacture: It is usually the C40, C45 steel structure, or alloy steel 40Cr. In case of the large load for the important machine, the used material can be Chromium - Manganese steel material such as 35CrMnV, 40CrMnTiBo, and Chromium-Nickel steel 40CrNi; 45CrNi, 30CrNi3A, etc. which are improved and hardening by high-voltage electricity at center shaft surface and antifriction working surfaces.

1.1.2. Working condition of the shaft: Imparting vertical torque moment of the axis from the above element to others or implementing of both above duties.

1.1.3. Basic damaged forms of the shaft

- Damaged by fatigue: Due to the high impact of the shaft, with a certain and long-term cycle, during the working process, the center shaft may cause fatigue, causing cracks, surface flakes, etc.

- Damaged by abrasion: Due to the relative movement of the center shaft and bearings, the center shaft is in abrasion, leading to changes in shape, size, and surface quality.

1.1.4. Operation of reinstated machine elements

In general, the reinstated machine parts are required to be in accordance with the quality indexes of the new ones. In fact, the use of machine elements that are reinstated by different methods may not ensure the quality, in detail:

+ Not enough durability, causing damage when working under a large load; Abrasion, changing the geometry of machine details and their relative position accuracy; Deformed metal destroying the outer surface layer and causing cracks, mudguard, etc.;

It can be seen that the operation, as well as the long life of reinstated machine elements, are determined by three main criteria: the bonding strength between the welding surface and the basic axis surface, wear resistance and fatigue strength.

1.1.5. Restoring methods of shaft machine parts

There are many methods to restore machine parts; however, each method has specific characteristics, providing the effectiveness and reinstatement quality.

a) Restoring of the abraded shaft by using welding technology

It is a technology applied widely to reinstate abraded and damaged details. This method helps restore the shape and dimension of the machine details. In many areas in the world, damaged details that are restored by welding method account for 60% - 70%. In our country, welding technology is popular, providing good quality and high economic effectiveness.

Machine details restoring by welding is characterized by its ability to restore many abraded and damaged forms (crack, mudguard, high abrasion). The welding equipment is simple, easy to transport. Inter-strength durability of the hardfacing layer of the substrate is good.

b) Restoring of damaged parts by using thermal spraying technology

Restoring of shaft surface by using thermal spraying technology is specialized by the axis with the metal coating thickness of 0.2÷6mm. The shafts surface is not burned at too high temperature, avoiding changes in metallography structure, transformation, being able to spray metal into the axis surface made of any material and diameter. However, it is a weakness that this method requires advanced technique, complicated equipment, and high cost. The amount of sprayed metal is in large losses, the fillet welding metal often has many pores and contains a large amount of oxides, and the wear resistance of the metal is very poor in dry friction working conditions, hazardous work environment.

c) Restoring of the abraded shaft by using coating technology

Restoring of the element by using plating technology is used widely to restore axis surface of low abrasion. In plating, the axis surface is not burned at too high temperature, not changing the structure and properties of metal of the shaft; the excess for manufacture is very small in comparison with welding methods. Plating hardness depends on the plating condition and metal. This method has a big disadvantage that productivity of the process is too low, limiting the size of recovery details, not ensuring conditions, and working environment.

1.2. Research situation and use of restoration welding for shafts in the world and in Vietnam

At present, various reinstatement methods of abraded machine elements have been studied and applied. The main studies are based on a theoretical basis and advanced technical procedures to recover abraded machine parts such as methods of vibrating-electrode welding, induction welding, sub-merged welding, gas welding, plasma welding, and explosion welding, reinstatement by diffusion welding, etc. Although these methods have many advantages, there are also existing disadvantages. For example, in their use to restore the cylindrical surface of the axis with low abrasion, it was shown that these methods do not always ensure the reinstatement quality of machine elements as required. In terms of the thermal spraying technology, which is used quite a lot, it has many outstanding advantages; however, this technology also has the disadvantages related to bonding strength of the coating with the low basic substrate. The amount of metal when spraying is with large losses, high porosity, creating a lot of metal oxide, bad working environment.

Advanced methods, which are constantly improved, for element reinstatement is resistance electric welding on the basis of using thermal energy produced when forming a weld between the filler material and the basic element when it is transmitted through the contact surface of an electrical impulse (Joule's law) combined with the electrode roller. These methods have many advantages over the reinstatement method based on the melting of filler materials by electric arc energy. The most important points in this method are:

- + The heat-up the parts is small
- + Welding ability of different filler materials;
- + The surface layer is tempered and forged directly in the welding process in order to increase the durability of the parts, so the element after welding only needs to be manufactured for the size and surface roughness without thermal treatment. As a result, it will avoid phenomena such as peeling and deformation, etc.;
- + The performance is increased by twice or three times;
- + Material consumption is decreased by three to four times in comparison with other welding methods;
- + It avoids burning and damaging of compound metal and helps better working conditions.

Conclusion for Chapter 1

Through studying on domestic and world research works on restoring by hardfacing technology and resistance seam welding technology for restoration of abraded shaft parts, it can be concluded with some points as follows:

1. Numerous welding technology are studied relatively comprehensive and they are applied into practice to restore wore parts. Amongst these technologies, the resistance seam welding technology for reinstatement of shaft components has been investigated since the 1970s and widely applied in the field of restoring agricultural mechanics machine elements in the Russian Federation. There has been no significant domestic study as well as application of this technology in spite of the fact that as per studies, it is indicated that this technology provides various strengths such as high productivity in welding procedure, ensured working environment, good wear resistance of hardfacing layer, high bonding strength, ability to weld dissimilar materials in which filler wire made from steel is more commonly used because it has a lower cost than metal powder. Therefore, it is necessary to study and complete this method for manufacture, repair, and statements in our country

2. The studies pointed out that the bonding strength of hardfacing layer in comparison with the basic metal, wear resistance and hardness of welded layer are the three most important features which influence the working ability of restored machine elements. In particular, regarding resistance seam welding technology for reinstatement of machine elements, the bonding strength of welding layer is put in priority because welding connection is only for the quasi-liquid status of welding metal and a basic substrate metal. Hence, the study on technological parameters for enhancement of this standard is one of the most must-do duties.

3. The objective and scope of the study are identified, in which it focuses on the simultaneous influence of technological parameters towards quality indexes of welding connection in resistance seam welding technology for reinstatement of shaft machine parts with the steel wire as filler material.

CHAPTER 2. THEORETICAL FOUNDATION OF RESISTANCE SEAM WELDING TECHNOLOGY FOR RESTORATION OF THE SHAFTS

2.1. Theoretical foundation of resistance seam welding

2.1.1. Definition, features, and application of resistance electric seam welding

Definition: resistance electric welding is a pressure welding procedure, using thermistor through the contact surface of two welding elements in order to melt metal to the welding status (quasi-liquid status) and welding the two workpieces by compressing forces. The metal of welding surface will be in mutual diffusion and osmosis, creating the welding joint.

+ Features of resistance electric welding

The current intensity is extremely high; effect duration is short; it is unnecessary to use welding flux or protective gas; the weld is in high quality without any slag; welding procedures obtains high productivity, giving a low number of deformed elements; it is easy to mechanize and automatic in welding procedure.

2.1.2. Resistance seam welding

a) *General principles:* Seam welding or roller welding is a type of resistance welding in which the welds concentrate on the constant welding spot. Electrode welding is in the shape of a wheel (active or passive, but required at least an active wheel), when kept between the two-wheel, so the weld is a closed line without any trespass of liquid and gas (Figure 2.1)

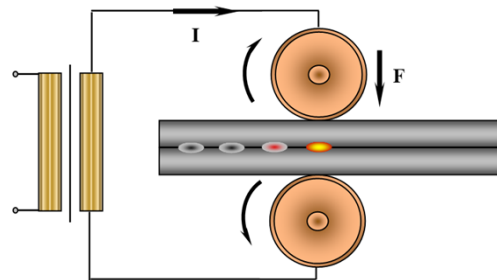


Figure 2.1. Principals of resistance seam welding

b) *Methods of resistance seam welding:* There are three methods of resistance seam welding as follows:

- Continuous seam welding (Figure 2.2-a).
- Intermittent seam welding (Figure 2.2-b).
- Step welding (Figure 2.2-c).

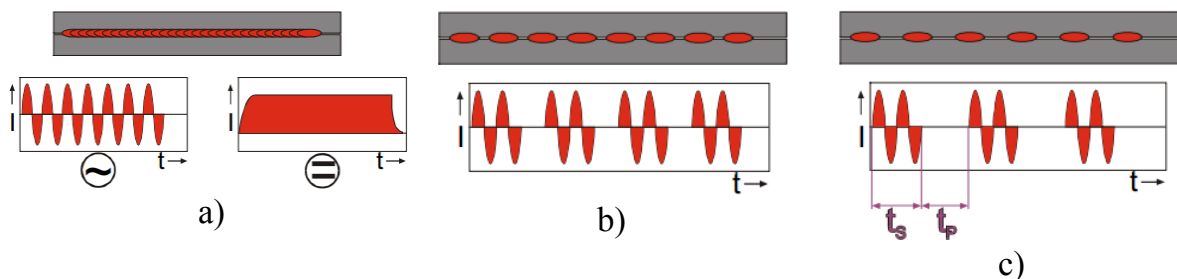


Figure 2.2. Methods of resistance seam welding

2.2. Methods of resistance welding for reinstatement of shafts

Based on the filler materials used, methods of resistance welding for reinstatement of machine elements are categorized as follows:

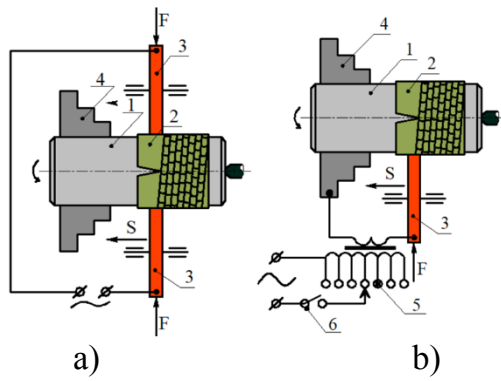
2.2.1. Resistance seam welding for reinstatement of shafts with steel strip filler material

Reinstatement diagram by resistance seam welding method with filler steel is present at Figure 2.3.

This method restores not only the outer cylindrical surface but also the internal cylinder clefts and surfaces. The recovery of shaft with keyhole, thin-walled parts by using resistance welding with filler materials of the steel strip is a high-economic and it is often un-practical by other methods. In order to ensure the quality of welded materials, it is necessary to use steel strips with a thickness of 0.25÷8 0.8mm from carbon steel, alloy steel and structural steel, rollers with a width equal to the width of the steel strip, weld resistance is at a level of less than or equal to 50 MPa.

Resistance seam welding for reinstatement with filler materials of steel strip still encounters some disadvantages.

+ The cutting of steel strips, surface grooving and mounting on restored surfaces may make the technical procedure complicated and limit the number of reinstated elements.



- 1- restored machine elements;
- 2- filler steel strip;
- 3- electric roller;
- 4- chuck;
- 5- welding transformer;
- 6- circuit breaker

a) 2-roller welding diagram; b) 1-roller welding diagram

Figure 2.3. Resistance seam welding for reinstatement of the shafts using filler steel strip

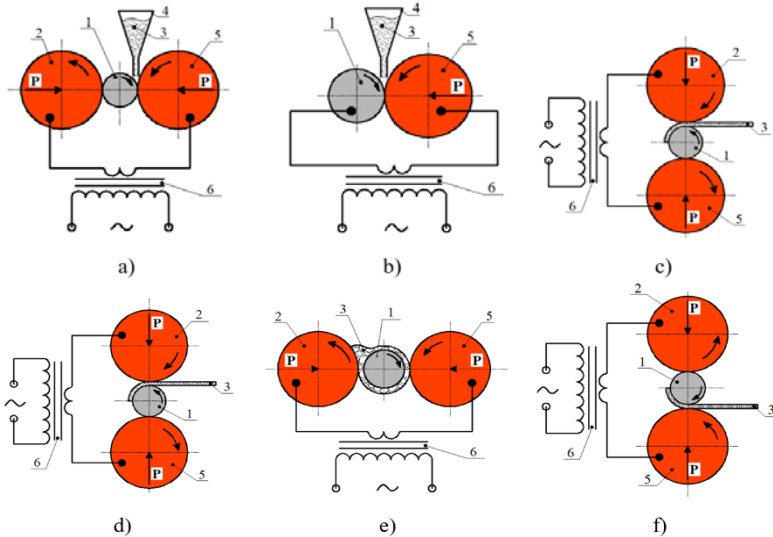
+ In case of welding in the optimal conditions, it is difficult to remove defects such as porosity, cracks, breakdown, and sloughing of the fillet-welded surface.

+ At the contact area of the filler steel strip and machine element, there is no plastic deformation of metal, which is considered as the essential condition for sustainable bonding.

Regarding the above-mentioned disadvantages, the use of contact welding method is limited.

2.2.2. Resistance seam welding for restoration of shaft with filler material of metal powder

It is indicated that there are many forms of using metal powder to create a weld when resistance seam welding with metal powder filler is used (Figure 2.4).



- 1- machine element for reinstatement;
 - 2,5- electric rollers;
 - 3- welding powder;
 - 4- funnel;
 - 6- welding transformer
- a- transferring powder by gravity through the funnel in 2-electric-roller welding;
- b- transferring powder by gravity through the funnel in 1-electric-roller welding;
- c- using sintered submerged fluxes;
- d- using polymer welding yarn;
- e- welding with pappy powder;
- f- powder associated with the surface.

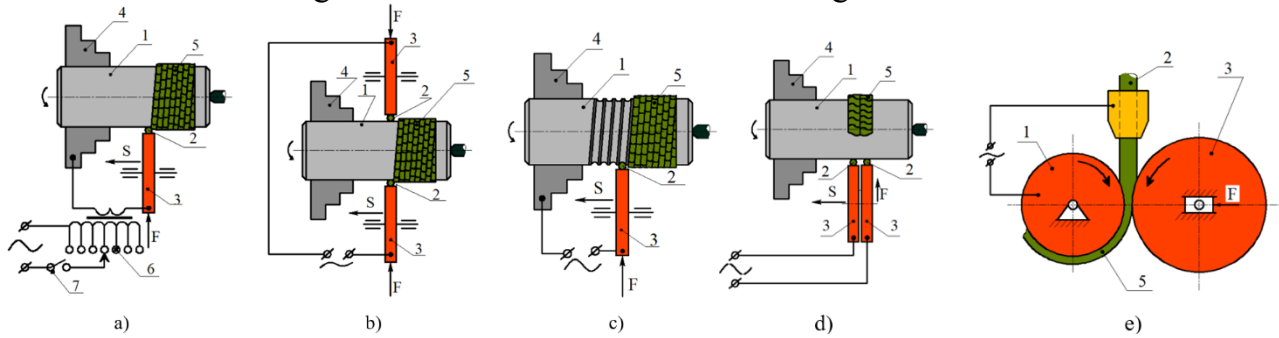
Figure 2.4. Diagram of contact roller-seam welding with metal powder use

Regarding contact welding method with metal powder, there are many options of welding powder (carbon and alloy), as well as different ways to combine them. It is possible to create a wide variety of components. The optimal mode in metal powder welding, ensuring the bonding strength of about 120 ÷ 150 MPa, the major factor affecting welding quality is its bonding with base metal, influencing welding speed, being an impact of temperature condition when welding coating layer. The porosity in the coating enhances the wear resistance. The fatigue strength of the machine axes is recovered by the resistance seam welding with metal powder which is insignificantly lower than using the metal steel strip welding.

Besides the advantages, a series of disadvantages exist in this method such as Large-sized electrode roller, the requirement of a working surface width equal to (or multiple of) the width of the restored axis neck (tenon-like axis). On welding, if a roller has a shorter width than the neck, the metal coating structure will be heterogeneous, saying because the welding procedure using metal powder is sensitive to temperature changes. The use of cheap iron powder does not always ensure the required reinstatement quality. The composition of welding materials complicates the technical process while high-quality alloy powders are rare and costly. The resistance seam welding with metal powder does not completely solve the problem of ensuring high bonding for the welding layer with the base metal of the axis. Then, the next mechanical processing steps of the coating in resistance seam welding with metal powder will encounter difficulties.

2.2.3. Resistance seam welding for restoring shaft with filler wire

Resistance seam welding with filler wire is described as in Figure 2.5.



1 – machine parts; 2- welding wire; 3- electrode for roller welding; 4- chuck; 5-metal coating;
 a- basic diagram; b- 2-roller diagram; c- creation of a cleft in the welded surface before welding;
 d- two adjacent rollers; e- Use of intermediate roller.

Figure 2.5. Diagram of resistance seam welding for reinstatement of the shaft with filler wire

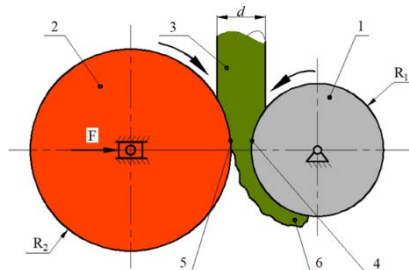
In addition to the above diagrams, there are many diagrams of resistance welding with metal wire; however, sometimes they are quite complicated and difficult to implement. In the technical documents, the author only obtained information on the application in the production of basic resistance seam welding diagram to restored abraded axes.

In this paper, the author used the basic diagram with changes: the electrode roller is pressed and shifted, the electric contact part on the welding axis also moves, so it gives the same electrical conductivity in the welding area, at that time, the supply current at the beginning and end of the welding section is unchanged.

2.3. Theoretical foundation of resistance seam welding process for restoration of shaft with steel filler wire

2.3.1. Principals of resistance seam welding restoration of shaft with steel filler wire

The principals of resistance seam welding procedure for restoration of shaft with steel filler wire are presented in Figure 2.6.



1 – welding axis;
 2 – electric roller;
 3 – metal filler wire;
 4 – contact surface of steel wire and welding axis surface;
 5 - contact surface of the metal wire and electric roller;
 6 – metal of welding layer.

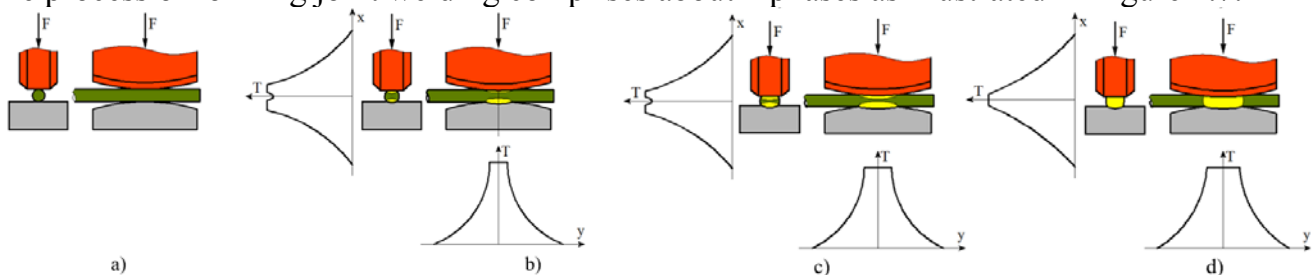
Figure 2.6. Diagram of Principals of resistance seam welding for reinstatement of shaft with steel filler wire

2.3.2. The physical essence of the metal bonding process

The formation of welding connection in resistance seam welding occurs without melting of base metal and filler metal. At the junction of base metal and filler metal, there is no formation of a welding tank. Resistance seam welding procedure is considered a variation of solid metal welding.

The width of the area forming a joint of welding wire to axis surface before impacting the electrical impulse will depend on the deformation resistance of the metal wire, the force of the electric roller, the diameter of the welding axis and welding filler wire, as well as welding surface conditions.

The process of forming joint welding comprises about 4 phases as illustrated in Figure 2.7.



a,b,c,d – phases of heating and plastic deformation of filler wire

Figure 2.7. Plastic deformation process of filler wire and temperature field of the welding area

2.3.3. Thermal balance in welding area formation

The thermal equilibrium equation in the formation of a welding point in resistance seam welding for reinstatement of shafts with steel filler wire can be constructed as follows:

$$Q = Q_{CT} + Q_1 + Q_2 + Q_3 \quad (J) \quad (2.1)$$

In which, Q_{CT} – the necessary amount of heat to melt a piece of metal between the shaft and the electric roller to the plastic state. Q_1 , Q_2 , Q_3 - the heat of the welding area passed into the welding shaft part, the roller electrode, and the welding filler wire after the time of an electrical pulse.

Amongst the four factors of thermal balance as shown in equation (2.1), the 2 factors of Q_1 and Q_2 move to the welding axis and electric roller, in other words, these 2 factors do not involve in the weld formation. Hence, they are called as heat loss components in the welding procedure. It can be concluded that energy efficiency index of the metal coating formation in roller welding is as follows:

$$\eta = \frac{Q_1 + Q_2}{Q} \quad (\%) \quad (2.2)$$

2.3.4. The relationship between plastic deformation ability of the filler wire to welding bonding strength

The relationship between non-dimensional strength of welding joint and relative deformation of welding wire is based on the element of vertical-axial deformation of the welding filler wire:

$$\bar{\sigma} = \sigma / \sigma_{\max} = k \cdot \varepsilon_y^m + C \quad (\text{MPa}) \quad (2.3)$$

$$\varepsilon_y = \frac{L_{dd} - L_{bd}}{L_{bd}} \quad (\%) \quad (2.4)$$

In which, σ - weld strength of coating with the base metal surface, MPa; σ_{\max} - limited strength of weld MPa; ε_y - relative deformation of the welding filler wire in the vertical-axial direction (L_{dd} - elongation of the welding filler wire measured after welding; L_{bd} – length of the welding filler wire measured before welding); k and m – experimental non-dimensional coefficient; C – fixed Non-dimensional integral.

2.3.5. Kinetics forming welding joint

The spread of the area forming this joint is completed after 0.020 ... 0.025 seconds. Time for heating to make plastic deformation with welding filler wire is 0.02 ÷ 0.06s. Nevertheless, $t_i = 0.04s$ is the time for the weld to be completely subsided and create the highest bonding strength.

2.4. Effect of technological parameters on welding layer quality

2.4.1. Effect of welding current (I_h)

It influences the thermal energy input of the welding procedure, welding productivity as well as the bonding strength of the welding layer with the basic welding shaft, besides I_h also affects other parameters of the welding procedure such as time of electrical impulses, electrode pressure force, etc.

2.4.2. Time of electrical impulse (t_i , t_n)

If the time of electrical impulse is too small, it is unable to ensure that the subsidence process of the filler wire is completed, the electrical impulse passing through the contact area does not cover the entire surface, at that time, bonding process occurs incompletely and it is the reason causing reduction of weld strength.

2.4.3. Effect of roller electrode pressure force (F)

Roller electrode pressure force creates initial physical contact. When electrical impulses run through the contact position, the metal filler wire is heated, quickly reaching the plastic state. At this moment, the pressure force maintains the subsidence of the secondary wire and then the welding connection is formed. The pressure force changes the contact resistance and the heat during welding.

2.4.4. Effect of welding speed (V_h)

The welding speed changes the heating time of the contact surface under the pressure force of the roller electrode. With high welding speed, the heating process may be not enough, leading to the deformation of burned area in process of loosening block stress. If welding speed is slow and proper, the bonding strength is lower than the maximum strength. It is because the welding surface is vertical to the shaft length and the coverage is high, causing reduction of intermediate contact resistance, current flow (bypass current).

2.4.5. Effect of welding progress (S_i)

If the welding progress is increased as per the spiral and over the proper scale, there is no overlap fillet-welding seam. If the welding progress as per the spiral is too low, it may strongly influence the

metal coating's structure. Simultaneously, it may increase the coating thickness of the adjacent welding seam and the width of the ream area. Consequently, the hardness and wear resistance of coating is decreased.

2.4.6. Effect of cooling water flow (Q_n)

By increasing the amount of cooling liquid and putting the liquid nearer welding area, it obviously reduces the effectiveness of contact electric welding procedure. However, the use of cooling water helps enhance the hardness of the fillet welding metal layer.

In terms of impact analysis of I_h , F , V_h , t_i , t_n , S_t , Q_n , it is determined that parameter of the cooling water flow Q_n is the one to enhance the hardness of welding surface. Electric impulse welding parameters t_i , t_n were pointed out in some studies that the optimal level for 1.8mm welding wire is $t_i = 0.04s$; $t_n = 0.08s$. Basically, S_t is to ensure the recovered area and anneal area. The other parameters including I_h , F , V_h are the ones directly changing thermal energy, weld formation mechanism. As a result, they are studied and selected as the control parameters in the experiment.

Conclusion for Chapter 2

1. In high productivity of welding procedure, welding workpiece will be less deformed due to the use of electric current with huge intensity in a short time. In welding, it is not required any welding flux or protective gas, the weld is without any slag, so working conditions and the environment is good. Additionally, the method provides high-quality weld and easily automatics in the welding procedure.

2. On the basis of physical properties of resistance seam welding for restoring of shafts, it can be concluded that this method is one of resistance welding by pressure force. The weld is formed in high plastic flow temperature, which means there is no flux of welding and base metal. Kinetics for connection development of welding and substrate metal is defined by their kinetics of plastic flow deformation. Therefore, the welding joint is not fired or its alloy elements are not evaporated. Chemical element change of welding and substrate metal has little and insignificant influence. Consequently, the restored shafts can obtain a surface with high hardness and good wear resistance, ensuring its plastic strength. The formation process of welding joint mainly occurs in the contact area; hence, dissolubility of base metal into the welding metal is lower, contributing good purity of the fillet layer, high and homogeneous average hardness.

3. The study presented that in the weld formation under solid phase, the relationship of bonding strength between welding metal and base metal was understood through the deformation of metal wire in welding. The paper also analyzed and reviewed the effects of basic welding parameters toward the welding j quality. Moreover, it serves as a base to narrow down and select suitable technological parameters for experiments.

CHAPTER 3. MATERIALS, EQUIPMENTS, EXPERIMENTAL METHODS AND EVALUATIONS

3.1. Experimental model

The experimental model is built on the input bases of the process and the output targets after the recovery welding, this model is described in Figure 3.1.

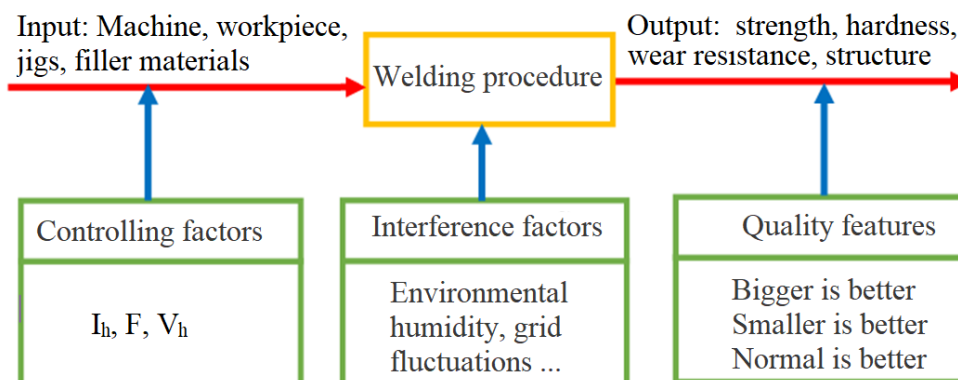
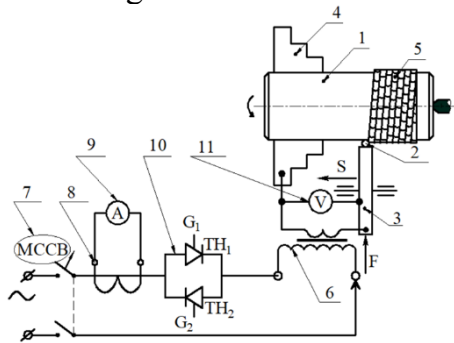


Figure 3.1. Experimental model

3.2. Experimental equipment and materials

3.2.1. Experimental equipment

The experiment of recovery resistance seam welding technology to restore shaft parts with steel filler wire, the author uses ARO 72500 ARO 72500 welding machine produced according to NF A 82-020 standard of France in combination with manufacturing fixture to create the diagram like Figure 3.2 and images as shown in Figure 3.3.



- 1- welding recovery axis; 2 - metal filler wire ; 3 - roller electrodes; 4 - chuck; 5- welding layer; 6-transformer; 7- Automatic circuit breaker; 8 - current transformer; 9 - ammeter; 10- Thyristors installed in parallel, 11- voltmeter

Figure 3.2. Circuit diagram and electrical test equipment



Figure 3.3. Recovery resistance seam welding of shaft parts

3.2.2. Experimental materials

3.2.2.1. Materials selection and process the experimental samples

+ Experimental welding sample is made of high-quality C45 carbon steel. The shaft with a nominal diameter of 100mm has worn 1mm in diameter, i.e. the experimental welding axis is 99mm in size. After the recovery welding with two welding layers by resistance seam welding technology and mechanical processing, the axis comes back to the original size of 100mm. Experimental chemical and mechanical properties are tested at the Laboratory of High-Performance Materials - Institute of Energy and Mining Engineering - VINACOMIN as shown in Tables 3.1 and 3.2.

Table 3.1. Chemical composition of experimental samples (%)

C	Si	Mn	P	S	Cr	Ni	Cu	Mo	Fe
0,4708	0,2630	0,6570	0,0271	0,0078	0,0743	0,0396	0,0178	0.0041	98,3808

Table 3.2. The tensile test results of the fabrication material of welding shaft and drawing pins

Experimental norms	Unit	Results			
		Sample 1	Sample 2	Sample 3	Average
Limit of tensile strength	N/mm ²	495	485	484	488

+ To assess the bonding strength of the welded layer with the basic shaft, the study uses the separation of Ø4 diameter cone-shaped pins from the welding layer. A sample of welding shaft and drawing pin is designed, manufactured, and assembled as shown in Figure 3.4. and 3.5

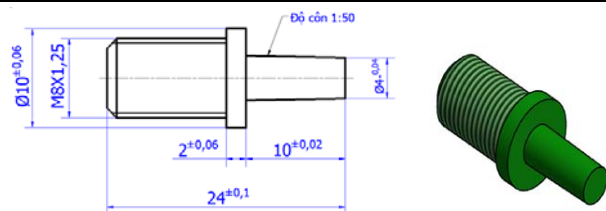
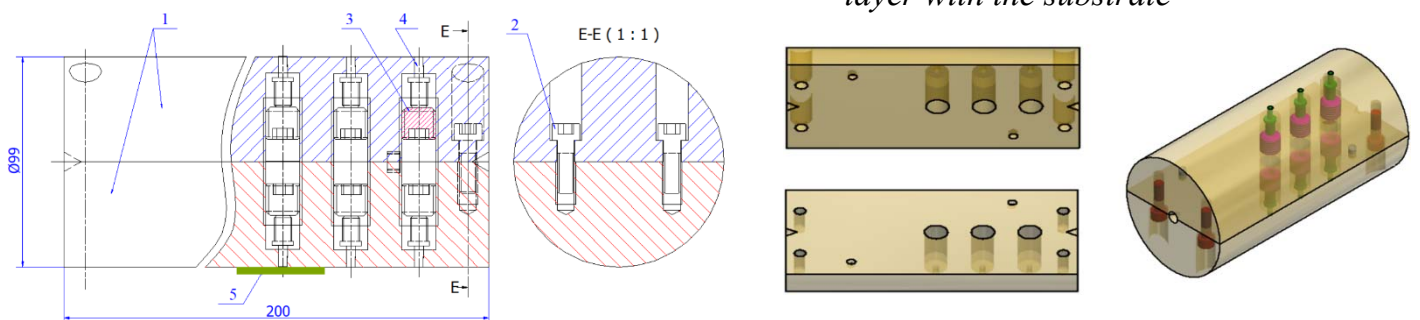


Figure 3.4. Durable checking pin joints the welding layer with the substrate



1 - 2 halves of welding sample; 2 - screws; 3 - blocking button; 4 – cone-shaped pin; 5 - welding layer
Figure 3.5. Assembly model of the experimental sample

3.2.2.2. *Choose material of welding wire*

Selecting material of 1.8mm diameter C70 steel wire as welding wire material for the experimental process of recovery resistance seam welding technology of shaft parts. Materials of welding wire are tested for chemical composition at VINACOMIN Institute of Energy and Mining Engineering as Table 3.3.

Table 3.3. *The chemical composition of welding filler wire(%)*

C	Si	Mn	P	S	Cr	Ni	Cu	Mo	Fe
0.6720	0.1760	0.5270	0.0057	0.0063	0.0435	0.0275	0.0485	0.0033	98.4720

3.3. Experimental planning method

3.3.1. Taguchi Experimental design method

The combination of factors affecting the objective function is done through L9 orthogonal arrays. The test results are analyzed by statistical method via signal/noise ratio (S / N).

3.3.2. ANOVA analysis of variance

Quantifying the relative influence of factors and the importance of experimental parameters on the objective function

3.3.3. Multi-objective optimization based on combined analysis of the relationship between Grey and Taguchi

In this thesis, the author uses relationship analysis (GRA) to determine the optimal value of welding technology parameters I_h , F , V_h , to the bonding strength of welding layer with substrate, hardness and wear resistance of the welding layer includes the following steps:

Step 1: Experimental design

Step 2: Grey relationship analysis includes: Standardization of experimental data; Calculation of Grey relation coefficients; Calculation of the level of Grey relationship; Analysis of the relationship between Grey and Taguchi

The optimal level of process parameters is the highest level of Grey relationship value.

3.4. Method of testing and evaluating welding quality

3.4.1. Study the composition of the welding layer structure

Evaluate the appearance of the welding layer - with a magnifying glass, a caliper.

Evaluate the structure of welding joint includes: unrefined welding structure; microstructure of the welding layer, contiguous areas of welding metal with the substrate, heat-affected area - on Axiovert 40 MAT optical microscope equipment.

Evaluate the chemical composition of welding - by using Metal Lab 75/ 80J MVU-GNR emission spectral ray apparatus.

3.4.2. Mechanical testing method of welding layer

Evaluate the bonding strength of welding layer with the substrate by separating the cone-shaped pin from the welding layer - on the WEW tensile testing machine 1000B

Evaluate the hardness of welding layer on the HPO-250 hardness tester

Evaluate the cross-section hardness of welding joint on 401-MVD-Wilson Wolpert micro hardness tester

Evaluate the metal wear of welding layer on TE97- Friction tensile strength measuring device

Evaluate the wear resistance of the recovery-welding shaft with the new C45 high frequency steel shaft and the hardness through the abrasive strength-measuring device and structure the abrasive SEM shooting.

3.5. Experimental exploratory process

3.5.1. Selection of parameters of technology mode welding parameters

On the theoretical basis presented in chapter 2 and the initial exploration experiments for the purpose of equipment testing and technology implementation showed that the welding was formed in the range of technological parameters: $I_h = 5.5 \div 9 \text{kA}$; $F = 1.5 \div 2.5 \text{kN}$; $t_i = 0.02 \div 0.06 \text{s}$; $t_n = 0.06 \div 0.08 \text{s}$; $V_h = 1.5 \div 2 \text{cm/s}$; $S_t = 1.5 \div 2.5 \text{mm/round}$.

3.5.2. Some experimental results of exploration

a) Macrostructure results

Conduct welding 3 samples Geology 1: $I_h = 8.5 \text{kA}$; $F = 2.3 \text{kN}$; $t_i = 0.04 \text{s}$; $t_n = 0.08 \text{s}$; $V_h = 2 \text{cm/s}$; $S_t = 2.5 \text{mm/round}$; Geology 2: $I_h = 7.5 \text{kA}$; $F = 2 \text{kN}$; $t_i = 0.04 \text{s}$; $t_n = 0.08 \text{s}$; $V_h = 1.75 \text{cm/s}$; $S_t = 2 \text{mm/round}$; Geology 3: $I_h = 6.5 \text{kA}$; $F = 1.7 \text{kN}$; $t_i = 0.04 \text{s}$; $t_n = 0.08 \text{s}$; $V_h = 1.5 \text{cm/s}$; $S_t = 1.5 \text{mm/round}$; The cooling water flow of all 3 samples is $Q_n = 1 \text{ liter / minute}$, and provide with the results as shown in Figure 3.6.

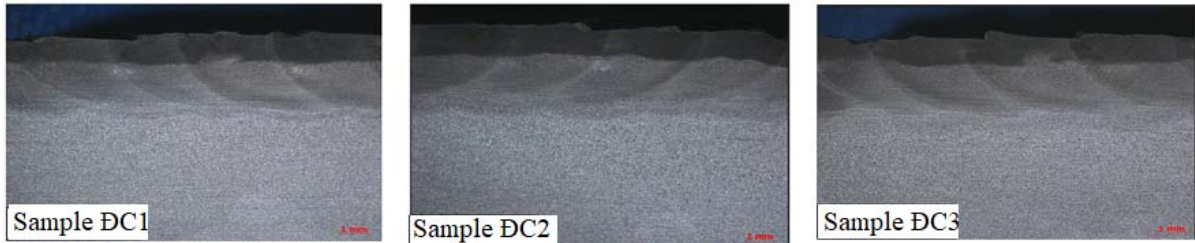


Figure 3.6. Macrostructure of welding exploratory samples (16x)

The photo result of the macrostructure of the welding shows the very good bonding of the welding metal to the base metal, the first welding layer with the second welding layer, the metal bonding after each electrical impulse.

b) Results of bonding strength of the welding layer with the substrate

The evaluation process of the bonding strength of metal layers with basic axis metal samples with welding mode as in item (a) has resulted in table 3.4.

Table 3.4. The exploratory tensile strength of the welding layer and base substrate

Experimental norms	Unit	Results		
		Sample 1	Sample 2	Sample 3
Tensile strength	N/mm ²	398	406	390

c) The hardness of the covered metal layer

The hardness test results of 03 samples with test results in Table 3.5 are the average results of 5 measuring points.

Table 3.5. Hardness test results of exploratory samples

Samples	Sample ĐC1	Sample ĐC2	Sample ĐC3
Average value (HRC)	51	47	45

As shown in section 3.5.1 when welding with technological mode parameters: $I_h = 5.5 \div 9 \text{ kA}$; $F = 1.5 \div 2.5 \text{ kN}$; $t_i = 0.02 \div 0.06 \text{ s}$; $t_n = 0.06 \div 0.08 \text{ s}$; $V_h = 1.5 \div 2 \text{ cm/s}$; $S_t = 1.5 \div 2.5 \text{ mm/round}$ the weld will be formed. However, through a number of exploratory experiments, it is shown that weld surface quality is stable with the parameters of the mode parameters: $I_h = 6.5 \div 8.5 \text{ kA}$; $F = 1.7 \div 2.3 \text{ kN}$; $t_i = 0.04 \text{ s}$; $t_n = 0.08 \text{ s}$; $V_h = 1.5 \div 2 \text{ cm/s}$; $S_t = 2.5 \text{ mm/round}$.

On the basis of theoretical analysis and results of exploratory experiments, the author selected the experimental welding parameters with different levels, to survey the parameter domain to achieve satisfactory quality criteria, are presented in Table 3.6.

Table 3.6. Experimental welding parameters

Technological parameters	Symbol	Unit	Level 1	Level 2	Level 3
Welding shaft diameter	D_t	mm	99	99	99
Welding wire diameter	d_d	mm	1,8	1,8	1,8
Welding current	I_h	kA	6,5	7,5	8,5
Electrode diameter	D	mm	220	220	220
Electrode pressure	F	kN	1,7	2,0	2,3
Time of electrical impulse	t_i	s (second)	0,04	0,04	0,04
Stop time of electrical impulse	t_n	s (second)	0,08	0,08	0,08
Welding speed	V_h	cm/s	1,5	1,75	2
Step along the spiral	S_t	mm/round	2,5	2,5	2,5
Flow of cooling water	Q_n	L/min	1,0	1,0	1,0

Summary

1. Resistance seam welding for restoring shaft part is based on the principle of resistance welding method of interrupted lines. Based on this awareness, an experimental model has been developed. The conduction of research on the method helps manufacture technology jigs that are suitable with research requirements, changing the function of exposed electric welding machine, connecting fixture system with welding machine at the mechanization level and high-level automation. The selection of suitable materials and methods for fabrication of experimental samples, welding materials help create welding layers to meet the set objectives of the research topic.

2. The research field is new in the technology of recovery welding in our country. Therefore, initial exploratory experiments have been conducted to find out the steps to implement and solve technology problems. It finds out the mode in which the device and technology form welds. On that basis, research and exploration will be continued to narrow the range of input technology parameters to obtain stable quality welds. It determines the value of the levels of the technological parameters: I_h (6,5; 7,5; 8,5 kA); F (1,7; 2,0; 2,3 kN) and V_h (1,5; 1,75; 2,0 cm/s) to conduct experiments.

3. It helps select devices to measure input parameters; equipment, research methods to evaluate the characteristics of quality of welding layer to achieve reliability.

4. The technology to restore shaft parts by resistance seam welding with steel filler wire are successfully implemented in the laboratory and can apply this technology to recovery production, manufacture new shaft parts.

5. It helps select Taguchi experimental design method with suitable orthogonal array (L9 array) for determining the experimental implementation plans, and apply ANOVA variance analysis to determine the reasonable and price treat the effect of technological parameters to the required performance criteria.

6. Methods are developed to assess the impact, determine the appropriate level of technological parameters to ensure simultaneous mechanical properties of the welding layer through the traditional analysis of Grey and Taguchi relations.

CHAPTER 4. EXPERIMENTAL RESULTS AND DISCUSSION

4.1. Results of the welding layer structure

4.1.1. Welding macrostructure

a) *The shape of welding surface:* The surface of the welds observed by eyes and magnifying glass showed that the welding layer made by the proposed method was quite stable. Welding scales are evenly arranged and have good adhesion; the recovery welding area ensures the required coverage (Figure 4.1).



Figure 4.1. Welding samples and experimental welding surfaces

+ When welding M3 sample with welding mode $I_h = 6.5\text{kA}$; $F = 2.3\text{kN}$; $V_h = 2.0\text{cm/s}$. This experimental sample is welded with low current, high pressure, and high welding speed. In other words, the welding sample has a low thermal impact (small I_h), short operating time; plastic deformation ability of the secondary wire is poor despite high pressure. It shows that the weld surface has a lower degree of thermal distortion, the welding seams in the spiral ring have incomplete weasel, and there is a separation in Figure 4.2.

+ When welding sample M8 with welding parameters $I_h=8.5\text{kA}$; $F=2.0\text{kN}$; $V_h=1.5\text{cm/s}$. It means the sample is welded with a high heat level for a long time and medium pressure. By observing the weld surface, it shows that the welding scales are evenly arranged, due to the large thermal deformation, these welding scales are directed against the direction of welding shaft. Welds have high adhesion, but the surface has scabbed scales in Figure 4.3.



Figure 4.2. Welding surface
M3: $I_h=6.5\text{kA}$; $F=2.3\text{kN}$;
 $V_h=2.0\text{cm/s}$

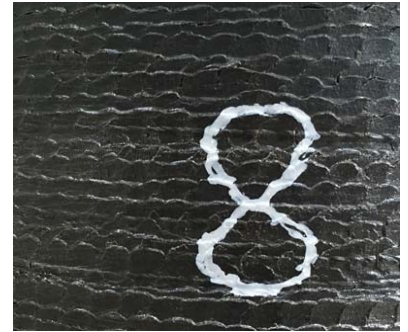


Figure 4.3. Welding surface
M8: $I_h=8.5\text{kA}$; $F=2.0\text{kN}$;
 $V_h=1.5\text{cm/s}$

b) *Macrostructure of the welds*

Macrostructure of the welds is tested and the results are in images on Figure 4.4.



M1: $I_h=6.5\text{kA}$; $F=1.7\text{kN}$; $V_h=1.5\text{cm/s}$



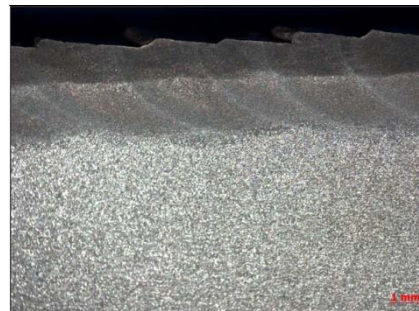
M2: $I_h=6.5\text{kA}$; $F=2.0\text{kN}$; $V_h=1.75\text{cm/s}$



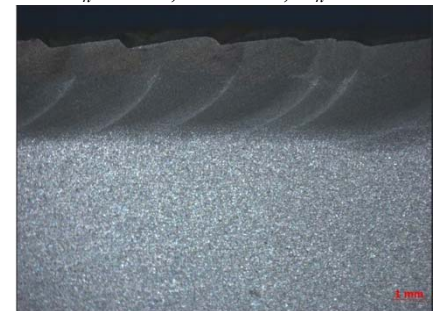
M3: $I_h=6.5\text{kA}$; $F=2.3\text{kN}$; $V_h=2.0\text{cm/s}$



M4: $I_h=7.5\text{kA}$; $F=1.7\text{kN}$; $V_h=1.75\text{cm/s}$



M5: $I_h=7.5\text{kA}$; $F=2.0\text{kN}$; $V_h=2.0\text{cm/s}$



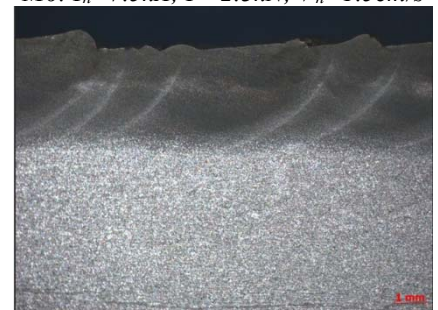
M6: $I_h=7.5\text{kA}$; $F=2.3\text{kN}$; $V_h=1.5\text{cm/s}$



M7: $I_h=8.5\text{kA}$; $F=1.7\text{kN}$; $V_h=2.0\text{cm/s}$



M8: $I_h=8.5\text{kA}$; $F=2.0\text{kN}$; $V_h=1.5\text{cm/s}$



M9: $I_h=8.5\text{kA}$; $F=2.3\text{kN}$; $V_h=1.75\text{cm/s}$

Figure 4.4. Macrostructure of experimental samples 16x.

+ Based on the shooting results of the welding *macrostructure*, it shows a relatively stable connection between two-layer welding metal, between welding metal to the base metal, between the welding layers after each welding pulse.

+ The binding areas have a clear distinction, the contiguous binding area, the narrow area of thermal influence.

4.1.2. Welding microstructure

a) *Welding microstructure*: is presented in Figure 4.5.

+ When welding with changes in welding parameters according to Taguchi experimental design of L9 array, it shows that the welding microstructures are quite similar. The image shows that the microstructure consists mainly of two main phases: needle-shaped martensite (dark color) and residual austenite (light color).

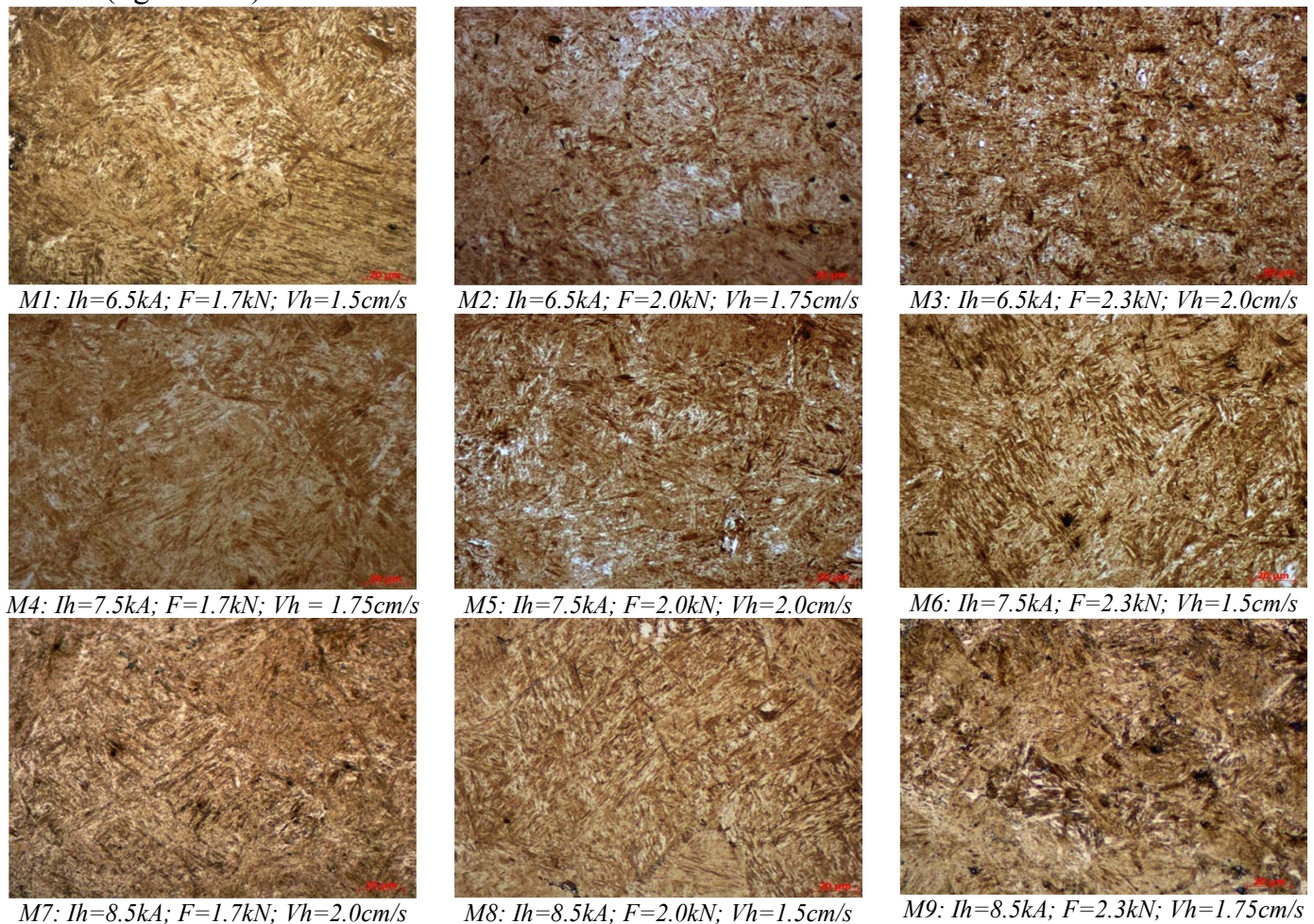


Figure 4.5. *Welding microstructure 500x*

The initial material structure consists of two light components, bright ferrite, and dark perlite, and structure after welding is needle-shaped martensite (dark color) and austenite (light color), due to thermal action during welding making phases of ferrite and perlite transforms into austenite phases. Immediately after that, the weld is quickly cooled by the cooling water flow, the cooling speed exceeds the annealing speed limit. Therefore, most of the austenite phases do not turn into a ferrite-cementite mixture on time, but only transform the shape variation from the austenite structure (center of the face) into martensite (the center of mass). The process of transformation and cooling is not continuous and complete, so in the welding organization, there is residual austenite (light color). Martensite structure is an unstable structure that occurs in welds, making its hardness and wear resistance significantly increased.

Martensite structure has a denser density in welding samples with large welding currents, slow welding speeds such as M7, M8 and vice versa such as sample M2, M3.

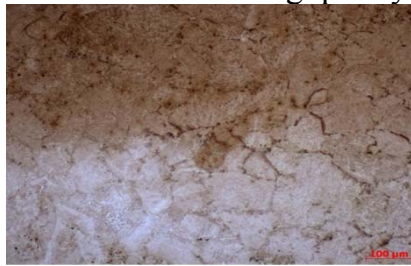
4.1.2.2. *The microstructure of the adjoining region between the welded metal and the base metal*

Through photos of the microstructure in Figure 4.6, it shows:

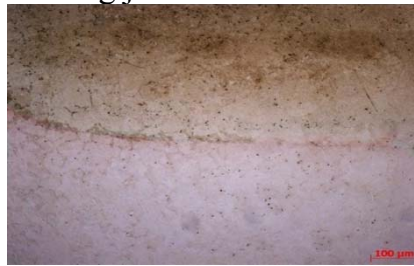
+ The contiguous metal area of the welding layer with the substrate metal shows that the welding samples have relatively good bonding, the welding area, and the base metal area is clearly distinguished.

+ Experimental welding samples show a metal transition between two contiguous areas for welding samples with high current, small pressure, and low speed. However, the stability of the bond is shown in experimental samples when welding with medium welding current (M4, M5, and M6). Welds with low current and high welding speed show that the bonding strength is not good, the contiguous area still has a clear demarcation line such as M2, M3. Welding samples with high current such as M7, M8, and

M9 show that the connection between the welding metal area and the substrate metal is also quite good. However, these samples have more black stains, especially in sample M8. This phenomenon can be explained by the reason that high current welding, low-speed heat, and excess supply with a great pressure will create a phenomenon of metal overflowing to areas not welded, splashing needle and that is a cause of deteriorating quality of welding joint.



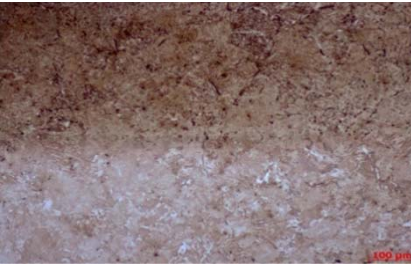
M1: $I_h=6.5kA$; $F=1.7kN$; $V_h=1.5cm/s$



M2: $I_h=6.5kA$; $F=2.0kN$; $V_h=1.75cm/s$



M3: $I_h=6.5kA$; $F=2.3kN$; $V_h=2.0cm/s$



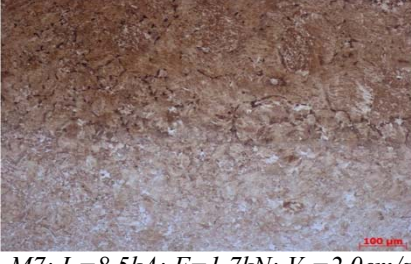
M4: $I_h=7.5kA$; $F=1.kN$; $v_h=1.75cm/s$



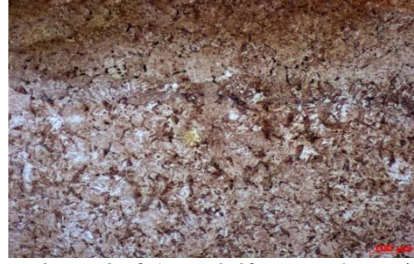
M5: $I_h=7.5kA$; $F=2.0kN$; $V_h=2.0cm/s$



M6: $I_h=7.5kA$; $F=2.3kN$; $V_h=1.5cm/s$



M7: $I_h=8.5kA$; $F=1.7kN$; $V_h=2.0cm/s$

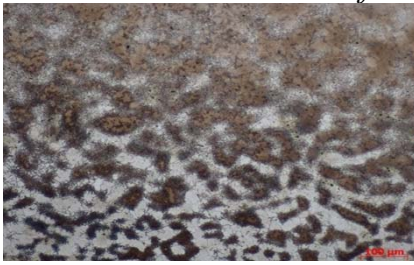


M8: $I_h=8.5kA$; $F=2.0kN$; $V_h=1.5cm/s$



M9: $I_h=8.5kA$; $F=2.3kN$; $V_h=1.75cm/s$

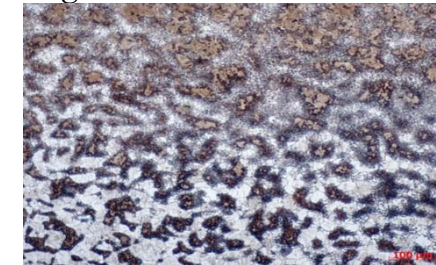
Figure 4.6. The microstructure of the region adjacent between the weld metal and the base metal
4.1.2.3. The microstructure of the base metal area adjacent to the welding metal



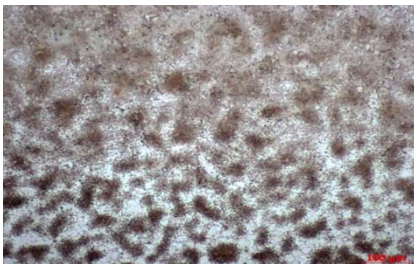
M1: $I_h=6.5kA$; $F=1.7kN$; $V_h=1.5cm/s$



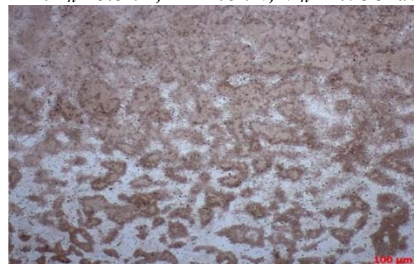
M2: $I_h=6.5kA$; $F=2.0kN$; $V_h=1.75cm/s$



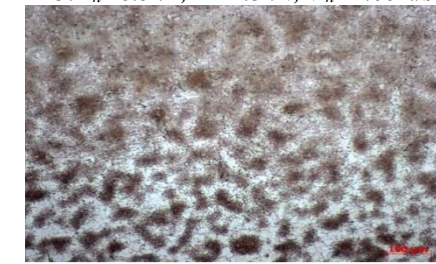
M3: $I_h=6.5kA$; $F=2.3kN$; $V_h=2.0cm/s$



M4: $I_h=7.5kA$; $F=1.kN$; $V_h=1.75cm/s$



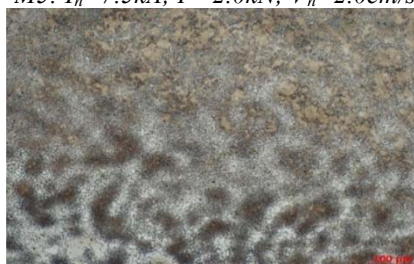
M5: $I_h=7.5kA$; $F=2.0kN$; $V_h=2.0cm/s$



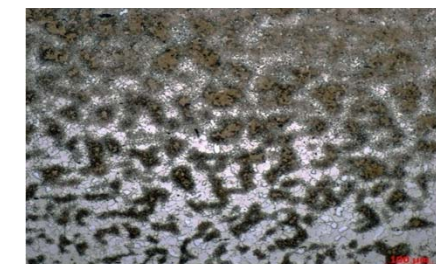
M6: $I_h=7.5kA$; $F=2.3kN$; $V_h=1.5cm/s$



M7: $I_h=8.5kA$; $F=1.7kN$; $V_h=2.0cm/s$



M8: $I_h=8.5kA$; $F=2.0kN$; $V_h=1.5cm/s$



M9: $I_h=8.5kA$; $F=2.3kN$; $V_h=1.75cm/s$

Figure 4.7. The microstructure of heat affected area

Through the Figure 4.7, it is shown that the structural change of the base metal related to the mode of heat supply. Specifically, the welding samples with low current and high-speed such as M2 and M3, the change of the basic metal surface structure has a small depth and when welding with high current, low speed, the structural change of the base metal surface has a greater depth (sample M7, M8).

4.1.3. Chemical composition analysis of welds

The chemical composition of the welds is analyzed and results are presented in Table 4.1.

Table 4.1. The basic chemical composition of welding sample after testing

Sample No.	Elemental composition (%)									
	C	Si	Mn	P	S	Cr	Ni	Mo	Cu	Fe
M3	0.5926	0.1550	0.4433	0.0097	0.0074	0.0503	0.0359	0.0053	0.0340	98.6369
M4	0.5871	0.1425	0.4364	0.0087	0.0069	0.0487	0.0345	0.0057	0.0353	98.6619
M8	0.5724	0.1405	0.4343	0.0081	0.0061	0.0484	0.0345	0.0057	0.0333	98.6859

The results of chemical composition analysis in Table 4.1 show that the main components such as carbon, magan, silicon are lower than that of welded metal components (Table 3.3). This can be concluded that diffusion, oxidation of elements occurs during the welding procedure, the level of oxidation increases when welding with high current and slow speed, i.e. the metal is affected at high temperatures for a long time.

Oxidation of elements is beneficial for mechanical properties of welds such as carbon, manganese, and silicon of exposed welding methods that occur at low levels. And it also shows the outstanding advantages of this recovery welding method compared to the recovery method by melting technology.

4.2. Results of welded mechanical properties

4.2.1. The bonding strength of welding layer with base metal

The result of bonding strength of welding layer with the substrate is the average value of three cone-shaped splits out of the welding layer on three different positions of the experimental welding samples

The bonding strength of welding layer with experimental shaft substrate by contact seam welding gives high and fairly uniform results, the results are evaluated through the snap-shaped surface after being removed from the welding layer (Figure 4.8) and test results are given in Table 4.2.



Figure 4.8. The surface of the cone-shaped pin removed from the weld

Table 4.2. The bonding strength of welding layer with base metal

No.	Sample name	Welding conditions			Tensile strength			
		I _h (kA)	F (kN)	V _h (cm/s)	1st (N/mm ²)	2nd (N/mm ²)	3rd (N/mm ²)	Average (N/mm ²)
1	Sample 1	6.5	1.7	1.5	422	446	454	440
2	Sample 2	6.5	2.0	1.75	422	414	438	424
3	Sample 3	6.5	2.3	2.0	390	374	414	393
4	Sample 4	7.5	1.7	1.75	470	470	462	467
5	Sample 5	7.5	2.0	2.0	438	446	454	446
6	Sample 6	7.5	2.3	1.5	430	446	454	443
7	Sample 7	8.5	1.7	2.0	430	438	446	438
8	Sample 8	8.5	2.0	1.5	446	454	454	451
9	Sample 9	8.5	2.3	1.75	422	430	438	430

+ The surface of the cone-shaped pin in Figure 4.8 shows the very high bonding strength of the welding metal with the substrate metal. These surfaces do not appear to have a surface separation, but a break with large undulations including base metal and welding metal.

+ When changing the values of welding technology parameters I_h , F , V_h , it shows the bonding strength of the welding layer with the substrate achieves different values. When increasing the welding current, reducing the pressure and reducing the speed, the welding strength tends to increase. Samples with low welding currents, pressure, and welding speed are at medium and high level, the bonding strength of welding layers with relatively low results (M2, M3) compared to other welding samples. When welding with medium welding current, low and medium pressure, the bonding strength of the welding layer with the substrate is the highest (M4, M5).

+ The results of the bonding strength of the welding layer with the substrate have also reflected the appropriateness through the images of macrostructure presented in Figure 4.4. The welding samples M4, M5, and M6 have a good transition between the covering layer and the base metal with good stability, while the samples M2 and M3 are somewhat less stable.

+ Based on the tensile strength value of base metal fabricated cone-shaped pin in Table 3.2 (with an average value of 488N/mm^2), compared with the result of the bonding strength of welding layer with the substrate when separating cone-shaped pins in Table 4.2 shows that the sample with the lowest bonding strength with the substrate is M3 393N/mm^2 reaching 80.5%, the sample has the highest bonding strength of welding layer with the substrate is M4 of 95, 7%. This ratio shows good advantages of recovery welding technology with exposed electric.

4.2.2. The hardness of weld metal

4.2.2.1. Hardness of welded metal surface

Hardness measurement results are performed on 05 different measurement positions on the surface of experimental welding samples, the overall hardness value of the experimental sample is the average value after 05 times as in Table 4.3.

Table 4.3. Hardness of welded metal surface

No.	Sample name	I_h (kA)	F (kN)	V_h (cm/s)	Measuring position					Average
					1	2	3	4	5	
1	Sample 01	6.5	1.7	1.5	51	54	53	52	53	53
2	Sample 02	6.5	2.0	1.75	48	47	50	51	49	49
3	Sample 03	6.5	2.3	2.0	45	47	48	48	49	47
4	Sample 04	7.5	1.7	1.75	49	53	53	50	51	51
5	Sample 05	7.5	2.0	2.0	50	48	49	51	54	50
6	Sample 06	7.5	2.3	1.5	53	49	54	52	53	52
7	Sample 07	8.5	1.7	2.0	54	51	55	54	55	54
8	Sample 08	8.5	2.0	1.5	55	56	53	54	57	55
9	Sample 09	8.5	2.3	1.75	52	49	53	49	54	51

+ When welding with high current, low welding speed, the weld is subjected to high heat and kept for a long time, the surface hardness increases to M1, M7, M8. In contrast, when welding with small current with high welding speed, small heat impact level, the weld hardness is lower than that of M2 and M3 although the C, Mn, Si components of M3 model are higher than M8 (table 4.1). This shows that surface hardening during welding procedure has a stronger effect than the loss of a small amount of C, Mn, Si components due to oxidation during the welding procedure.

With the selection of welding wire materials and the technological parameters of the experimental process show that the experimental samples all have quite high hardness, basically ensuring the general hardness requirements for the recovery details of $45 \div 55\text{HRC}$. Based on the obtained hardness results, most of the shaft parts do not need to be processed after welding, which is the greatest advantage that the technology brings, it will avoid thermal deformation, flaking welding layer due to post-welding heat treatment process can occur.

4.2.2.2. The hardness of cross-sectional welding metal

The result of weld cross-section hardness was assessed through the measured value in table 44, and the image of the stab in Figure 4.9.

+ Through the measured value and the image of the stab of the weld cross-section microstructure hardness, it shows the highest value metal area (small stab), corresponding to the nature of C70 metal wire, then is the heat-affected area (medium stab), the lowest is the substrate metal (large stab).

Table 4.4. The microhardness of cross-sectional welding metal

Hardness measurement (HV1)										
No.	Sample name	Welding area			Heat-affected area			Base metal area		
		Measuring position			Measuring position			Measuring position		
		1	2	3	1	2	3	1	2	3
1	Sample 3	461	452	395	325	257	225	214	195	191
2	Sample 4	481	466	378	307	296	261	214	196	193
3	Sample 8	496	482	405	327	249	216	213	191	185



Figure 4.9. Image of weld cross section hardness stab

4.2.3. Wear resistance of the welded metal

The amount of abrasion and abrasion strength of the welding samples checked and given the value in Table 4.5:

Table 4.5. Abrasion test results of experimental samples

No.	Sample name	I _h (kA)	F (kN)	V _h (cm/s)	ΔP (g)	n (round)	S (mm)	N (N)	I _m (g/N.mm)
1	Sample 1	6.5	1.7	1.5	0.0144	6160	580272	20	1.24080.10 ⁻⁰⁹
2	Sample 2	6.5	2.0	1.75	0.0164				1.41313.10 ⁻⁰⁹
3	Sample 3	6.5	2.3	2.0	0.0163				1.40451.10 ⁻⁰⁹
4	Sample 4	7.5	1.7	1.75	0.0150				1.29250.10 ⁻⁰⁹
5	Sample 5	7.5	2.0	2.0	0.0154				1.32696.10 ⁻⁰⁹
6	Sample 6	7.5	2.3	1.5	0.0148				1.27526.10 ⁻⁰⁹
7	Sample 7	8.5	1.7	2.0	0.0140				1.20633.10 ⁻⁰⁹
8	Sample 8	8.5	2.0	1.5	0.0143				1.23218.10 ⁻⁰⁹
9	Sample 9	8.5	2.3	1.75	0.0151				1.30111.10 ⁻⁰⁹

The abrasion resistance results of samples in Table 4.5 show that the wear resistance of the welding samples correlates with the welding layer hardness. Samples with high hardness such as M1, M6, M7, M8 have high wear resistance as well, samples with low hardness also have low wear resistance as well. Looking at Table 4.5, the samples with the highest hardness (M8) are not the ones with the highest wear resistance, while the sample M7 has the greatest wear resistance but not the highest hardness, the sample M3 has the lowest hardness but has higher wear resistance than sample M2. These reasons are explained by the welding layer structure cannot be as uniform as the casting structure, but also during the welding procedure, there are metal ram areas occurring after each axis twist.

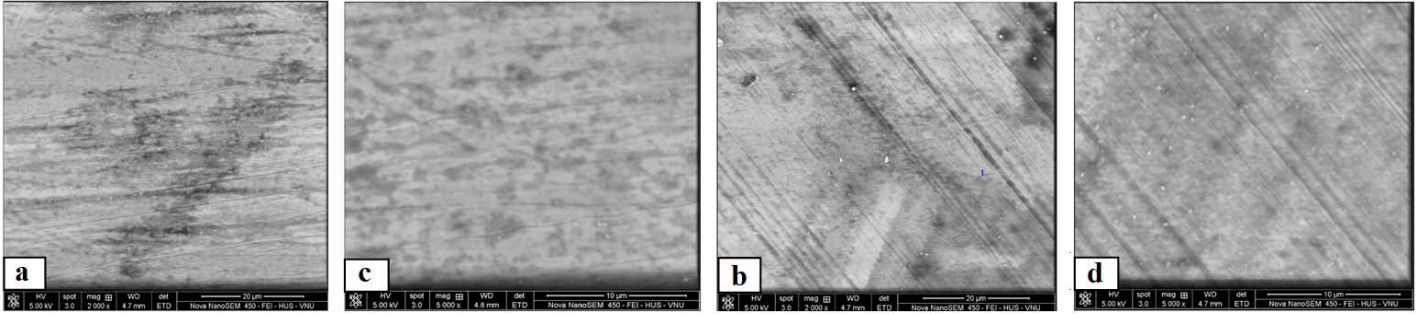
4.3. Evaluate the wear resistance of the recovery-welding shaft with the new shaft made from C45 annealed steel

To evaluate the wear resistance of the welded **shaft** to be restored by resistance seam welding with the C70 steel filler wire, by comparing the wear of the test piece separated from the welding sample with the test piece separated from the C45 high-frequency annealed steel sample of the same hardness. Test results of the wear resistance of C45 high-frequency annealed steel sample are shown in Table 4.6

Table 4.6. The wear resistance results of C45 high-frequency annealed steel sample

No.	Sample name	ΔP (g)	n (round)	S (mm)	N (N)	I _m (g/N.mm)
1	M 1c	0.0205	6160	580272	20	1.76413.10 ⁻⁰⁹
2	M 2c	0.0199				1.71471.10 ⁻⁰⁹
Average		0.0202				1.74056.10 ⁻⁰⁹

From the results table 4.5 and 4.6, it shows that the amount of wear of the samples taken from M7 welding sample has a hardness of 54HRC with a wear amount of 0.0140 (g), 1.44 times smaller than the average amount of wear samples from the C45 high-frequency annealed steel sample having the same hardness as the M7 sample. Welding samples with the lowest hardness are M3 with the wear amount of 0.0163 (g), also 1.24 times smaller than wear samples from C45 steel. This means that the wear resistance of the M7 sample is about 1.44 times and M3 is about 1.24 times higher than the C45 high-frequency annealed steel samples. The wear resistance of the welding metal layer reaches a high level, while the bonding strength of the layer with the substrate remains at about 80 ÷ 95% of the strength of the base metal. The results of evaluation of the wear of the welding sample and the high-frequency C45 steel sample are also shown through the SEM image in Figure 4.10. On the SEM image of the surface of the wear sample, it shows that the test piece taken from the high-frequency C45 steel sample has much larger abrasion and depth marks than from the wear sample from the M7 welding sample.



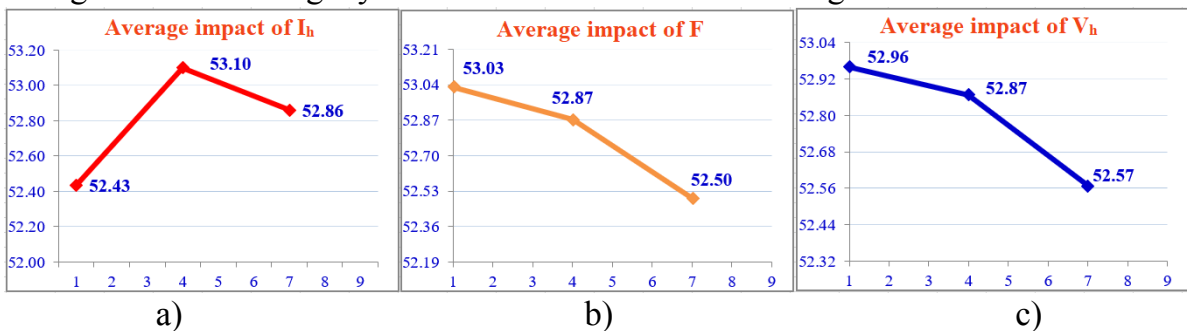
a,c- M7 welding sample with magnification of 2000x and 5000x; b,d- M1c sample with magnification of 2000x and 5000x

Figure 4.10. SEM image of the sample surface after the abrasion test

4.4.1. Effect and suitability of the technological parameters (I_h , F , V_h) to the bonding strength of the welding layer with the substrate

4.4.1.1. Determination of the impact rate and appropriate level of the technological parameters (I_h , F , V_h) to the bonding strength of the welding layer with the substrate

From the measurement results of bonding strength, the steps of Taguchi method and ANOVA analysis are performed, determining the appropriate level and percentage of influence of I_h , F , V_h on the bonding strength of the welding layer with the substrate shown in Figures 4.11 and 4.12.



a) Levels of I_h ; b) Levels of F ; c) Levels of V_h

Figure 4.11. Classification chart of factors for bonding strength of the welding layer with the substrate

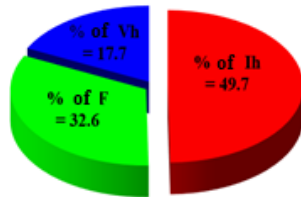


Figure 4.12. Chart of the influence level of the factors I_h , F , V_h on the bonding strength of the welding layer with the substrate

Based on the classification chart of the factors (Figure 4.11), it shows that: with the requirement that it is better to have greater quality, the appropriate level of the factors to achieve the greatest bonding strength when $I_h = 7.5$ (kA); $F_1 = 1.7$ (kN); $V_{h1} = 1.5$ (cm/s). When combining the factors (I_{h2} , F_1 , V_{h1}) in the process of experiments, the predicted value of the bonding strength of the welding layer with the substrate is as follows

$$Y_{opt} = T + (I_{h2} - T) + (F_1 - T) + (V_{h1} - T) = 471,22 \text{ (N/mm}^2\text{)}$$

From the distribution chart of the influence of welding parameters I_h , F , V_h on the bonding strength of the welding layer with the substrate (Figure 4.12), it shows the largest degree of influence of welding current is 49.7%; Next is the compression of roller electrode of 32.6% and welding speed of 17.7%.

4.4.1.2. Establishing mathematical relationships between parameters I_h , F , V_h , on the bonding strength of the welding layer with the substrate

Using the Minitab regression statistical software application of experimental data set between the bonding strength with the basic substrate with parameters I_h , F , V_h in linear form and power as follows:

+ Linear function form:
$$\bar{\sigma}_b = 513,7 + 10,33I_h - 43,9F - 38,0V_h \quad (4.1)$$

+ Power function form:
$$\bar{\sigma}_b = 375,316I_h^{0,183495} F^{-0,196231} V_h^{-0,14984} \quad (4.2)$$

Based on the linear regression function (4.1) and the power function (4.2) prepared, draw a chart showing the relationship of the welding metal bonding strength with the technological parameters. I_h , F , V_h , as Figures 4.13; 4.14; 4.15:

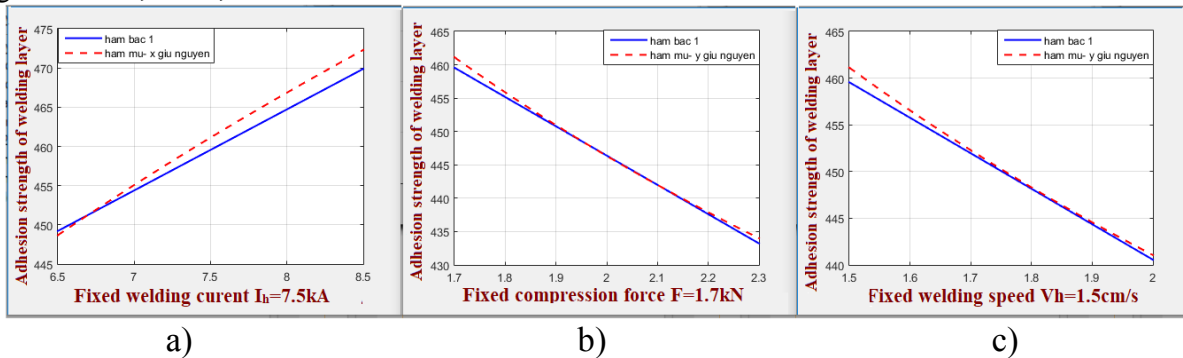


Figure 4.13. The dependence of the bonding strength of the welding layer with the substrate on the parameters I_h , F , V_h at the appropriate level in the form of 2D

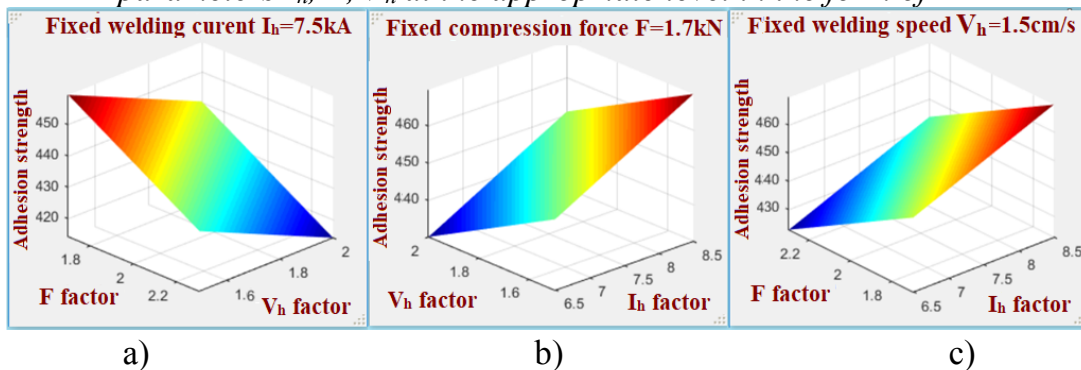


Figure 4.14. The dependence of the bonding strength of the welding layer with the substrate on the parameters I_h , F , V_h at the appropriate level of the linear function in the form of 3D

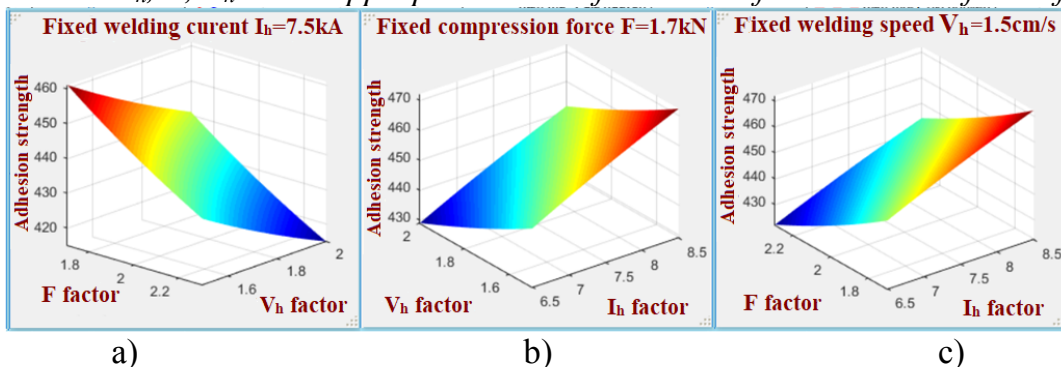


Figure 4.15. The dependence of the bonding strength of the welding layer with the substrate on the parameters I_h , F , V_h at the appropriate level of exponential function in the form of 3D

From the chart, it shows that the bonding strength of the welding layer with the shaft substrate is proportional to the welding current, which is inversely proportional to the electrode pressure and welding speed. This is equivalent to increasing the current strength, reducing the pressure and the welding speed, the bonding strength with the foundation will increase. This explanation is appropriate when increasing the welding speed, it will reduce the thermal impact and reduce the bonding strength. On the other hand,

when increasing pressure, it may occur excessive thermal deformation causing splashes, metal overflowing which hampers welding procedure and reduces the bonding strength of the welding layer with the substrate.

4.4.2. Effect and appropriate level of welding parameters (I_h , F , V_h) to welding metal hardness

4.4.2.1. Determine the impact rate and appropriate level of technological parameters (I_h , F , V_h) to welding metal hardness

Similar to the bonding strength, determine the appropriate level and the percentage of influence of I_h , F , V_h on the hardness of the welding layer as shown in Figure 4.16 and 4.17.

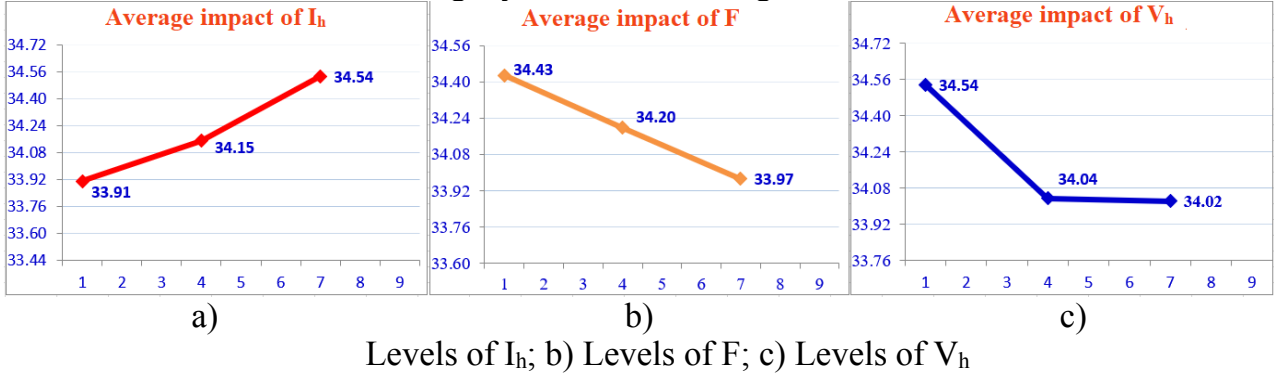


Figure 4.16. Classification chart of factors for the metal hardness of the welding layer

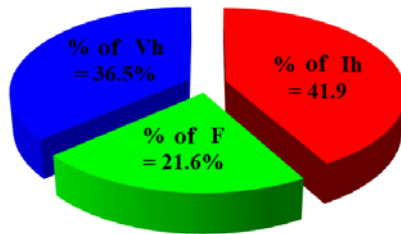


Figure 4.17. Chart of the influence level of the factors I_h , F , V_h to the hardness of the welding layer

Based on the results of the classification chart of the factors in Figure 4.16, it shows the appropriate level of the factors for the best hardness I_{h3} , F_1 , V_{h1} . The predicted hardness value when the combination of the factors is at the appropriate level for the welding hardness is at the highest level:

$$Y_{opt} = T + (I_{h3} - T) + (F_1 - T) + (V_{h1} - T) = 56,67 \text{ (HRC)}$$

Figure 4.17 shows that the influence of the factors on the strongest welding layer hardness is the welding current factor of 41.9%, followed by the welding speed of 36.5%, the smallest is the force of electrodes pressure of 21, 6%.

4.4.2.2. Establishing mathematical relations between parameters I_h , F , V_h to metal hardness of the welding layer

The same implementation is done with the bonding strength index with the base shaft substrate, giving the regression function as a linear function and a power function as follows:

+ Form of linear regression function: $R_w = 56,97 + 1,833I_h - 4,44F - 6,00V_h$ (4.3)

+ Form of power regression function: $R_w = 37,9002I_h^{0,268638} F^{-0,175556} V_h^{-0,211501}$ (4.4)

From regression expressions of 4.3 and 4.4, set 2D and 3D diagrams showing the relationship between the input parameters I_h , F , V_h , to the metal hardness of the weld of two types of interpolation functions such as figures below:

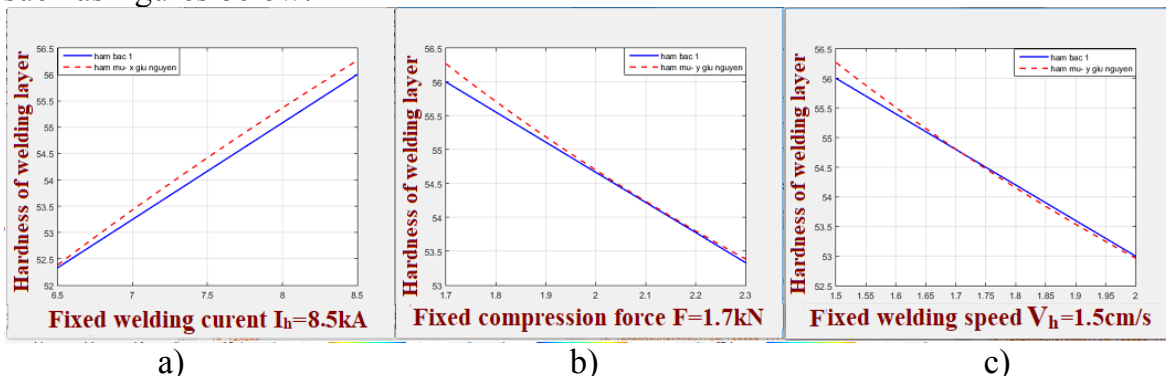
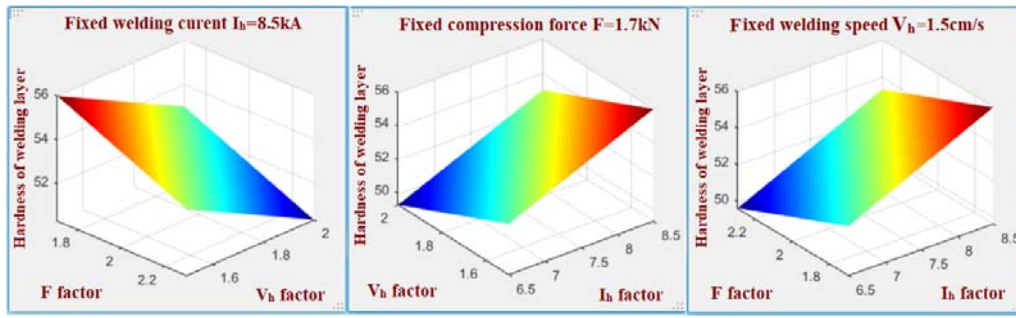
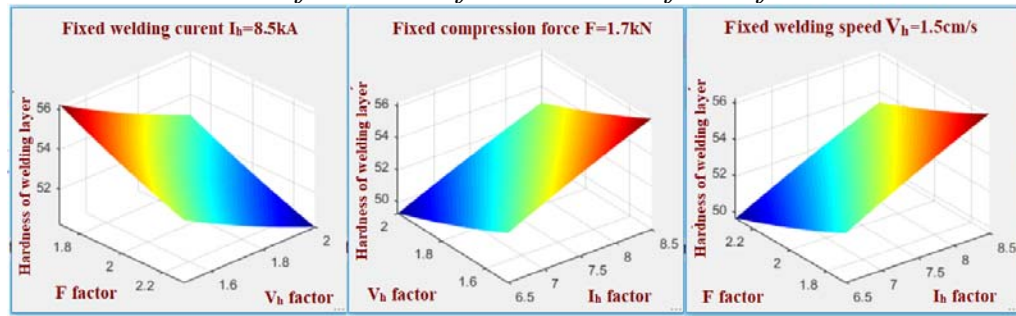


Figure 4.18. The dependence of the welding hardness on the parameters I_h , F , V_h at the appropriate level in the form of 2D



a) b) c)

Figure 4.19. The dependence of the welding hardness on the parameters I_h , F , V_h at the appropriate level of the linear function in the form of 3D



a) b) c)

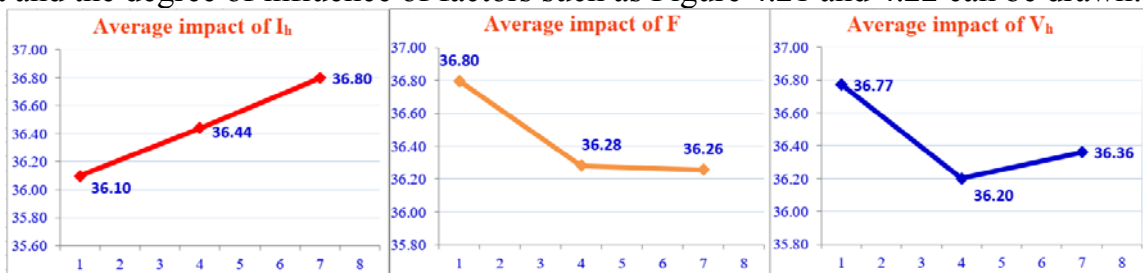
Figure 4.20. The dependence of the welding hardness on the parameters I_h , F , V_h at the appropriate level of exponential function in the form of 3D

From the chart, it shows that the hardness of the welding layer is proportional to the welding current, which is inversely proportional to the electrode pressure and welding speed. On the other hand, the two factors I_h and V_h are highly influential, which corresponds to an increase in the current and a decrease in the welding speed, which results in the metal being heated to high temperatures and faster cooling, creating the phenomenon of steel annealing and making welding metal increase the hardness. When the thermal impact density is high and the pressure outside adversely increases, apart from creating bad effects to the bonding strength of the welding layer with the substrate, it also mixes the base metal into the welding metal, reducing the purity of the welding metal and reducing the layer hardness.

4.4.3. Effect and appropriate level of technological parameters (I_h , F , V_h) to the wear resistance of welding metal

4.4.3.1. Determine the impact rate and appropriate level of welding parameters (I_h , F , V_h) to the wear resistance of welding metal

Based on the level and degree of influence of the factors on the abrasion of the welding layer, the level chart and the degree of influence of factors such as Figure 4.21 and 4.22 can be drawn:



a) b) c)

a) Levels of I_h ; b) Levels of F ; c) Levels of V_h

Figure 4.21. Classification chart of factors for welding abrasion to parameters I_h , F , V_h at the appropriate level in form of 2D

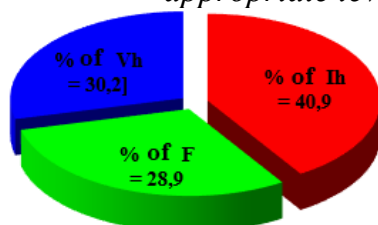


Figure 4.22. Chart of the percentage of effects of factors I_h , F , V_h on welding abrasion

The classification chart in Figure 4.21 shows that the smaller quality characteristic is better for the appropriate levels of the elements to have the smallest amount of wear, i.e. the maximum wear resistance with the levels of I_{h3} , F_1 , V_{h1} . The wear of the test piece with the smallest predicted value at the appropriate level is:

$$Y_{opt} = T + (I_{h3} - T) + (F_1 - T) + (V_{h1} - T) = 0,01328(g)$$

The classification chart of the influence of technological factors on the wear level of samples shows that the welding current parameter is still the strongest factor, the other two parameters have the same weighting effects. With the quality factor for abrasion, it shows that the influence of the technological parameters varies with the weld hardness. Specifically, in the hardness quality factor, F electrode has the lowest impact, while in this abrasive quality factor has greater influence than V_h , this is explained by the welding procedure of electrode pressing with a more flexible metal pressing effect (weld forging) which makes the structure of metal particles smaller, make the density of particles tighter, thus creating an impact on the wear resistance of welding metal to be better.

4.4.3.2. Establishing mathematical relationships between parameters I_h , F , V_h to the wear resistance of welds

The regression function represents the relationship of technological parameters to the wear resistance of the weld:

A form of linear regression function: $\Delta P = 0,01403 - 0,000617 \cdot I_h + 0,001556 \cdot F + 0,001467 \cdot V_h$
 (4.5)

Nonlinear regression form: $\Delta P = 0,021857 \cdot I_h^{-0,301792} \cdot F^{0,203271} \cdot V_h^{0,171057}$ (4.6)

Based on the mathematical regression function, drawing charts showing the influence of technological factors on the wear resistance of the welding layer as below:

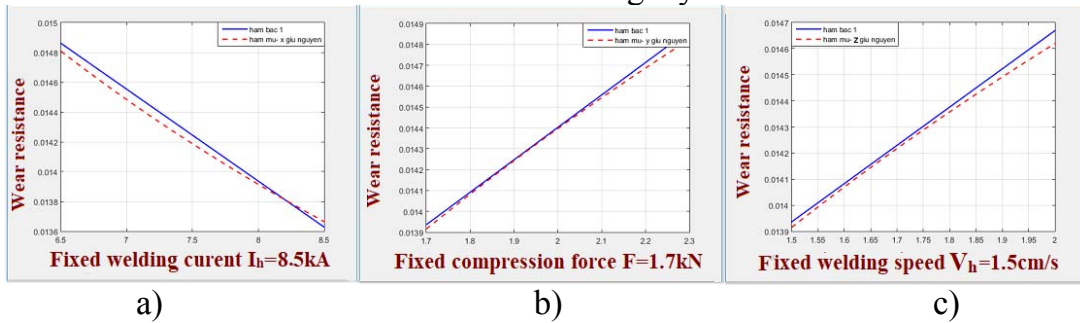


Figure 4.23. The dependence of the wear resistance on each welding parameter at an appropriate level in in 2D linear and exponential form

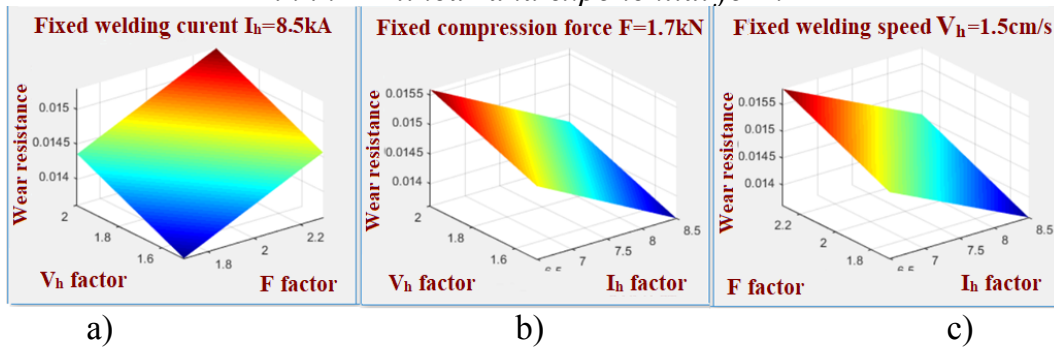


Figure 4.24. The dependence of the wear resistance of welding layer on parameters I_h , F , V_h at the appropriate level of linear function in form of 3D

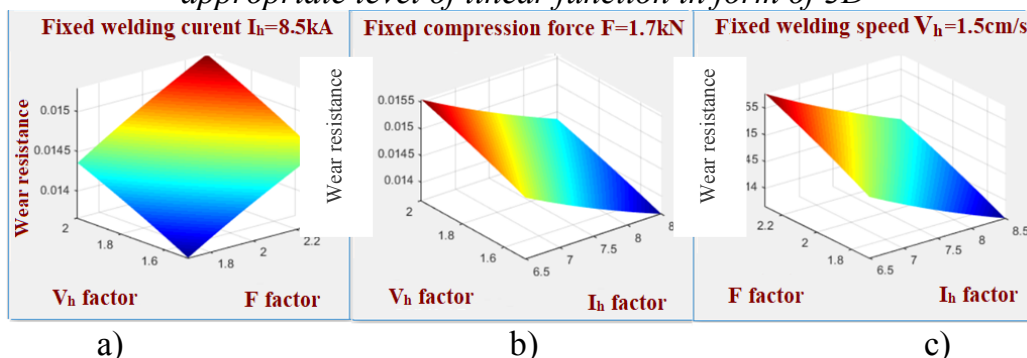


Figure 4.25. The dependence of the wear resistance of the welding layer on parameters I_h , F , V_h at the appropriate level of exponential function in the form of 3D

From the chart, it shows that the wear resistance of the welding layer is inversely proportional to the welding current intensity, i.e. the wear level will be high when the current is reduced, otherwise the wear resistance of the welding metal is proportional to the welding current, inversely proportional to pressure and welding speed, this is explained by high hardness samples, which are pressed at a suitable plastic flow temperature corresponding to relatively high wear resistance.

4.5. Evaluate the impact of technological parameters I_h , F , V_h according to the multi-objective optimization

The process of analyzing the hardness and wear resistance of the welding layer shows that the wear resistance of the welding layer is characterized by the quality equivalent to the hardness of welding layer due to the relatively high hardness samples giving the good wear resistance. The result for the set of technological parameters in accordance with the quality criteria is that the higher hardness, wear resistance are better than these of the same level (I_{h3} , F_1 , V_{h1}). Based on this meaningful analysis, the study selected and evaluated the influence of technological parameters I_h , F , V_h according to the problem of multi-objective optimization for two specific objectives: bonding strength of welding layer with the substrate and the hardness of welding layer, by Grey method combining Taguchi.

Implementing steps: Experimental design, standardization of data, Grey relationship analysis, Grey coefficient gives results as shown in Table 4.7.

Table 4.7. Results of Grey relationship analysis

No.	1	2	3	4	5	6	7	8
	Data normalizing measurement data		Standard deviation Δ_{oi} (k)		Grey coefficient $\xi_i(k)$		Grey level γ_i	Ratio S/N
	σ_b	R_w	σ_b	R_w	σ_b	R_w		
1	0.6351	0.7500	0.3649	0.2500	0.5781	0.6667	0.604688	-4.3694
2	0.4189	0.2500	0.5811	0.7500	0.4625	0.4000	0.443750	-7.0572
3	0.0000	0.0000	1.0000	1.0000	0.3333	0.3333	0.333333	-9.5424
4	1.0000	0.5000	0.0000	0.5000	1.0000	0.5000	0.850000	-1.4116
5	0.7162	0.3750	0.2838	0.6250	0.6379	0.4444	0.579885	-4.7332
6	0.6757	0.6250	0.3243	0.3750	0.6066	0.5714	0.596019	-4.4948
7	0.6081	0.8750	0.3919	0.1250	0.5606	0.8000	0.632424	-3.9798
8	0.7838	1.0000	0.2162	0.0000	0.6981	1.0000	0.788679	-2.0620
9	0.5000	0.5000	0.5000	0.5000	0.5000	0.5000	0.500000	-6.0206
max(Δ)			1.0000	1.0000				
min(Δ)			0.0000	0.0000				

The evaluation of the bonding strength of the welding layer and the weld hardness is based on the Grey level γ_i . The Grey relationship can be considered as an overall evaluation of experimental data for the bonding strength of the welding layer with the substrate σ_b and the hardness R_w . The hierarchy of correlation relationship is shown in Figure 4.26.

The quality factor is better when the Grey correlation coefficient is bigger, according to the chart in Figure 4.26, in the 9 experiments, there are 4 experiments that give better results than the experiment M4; M8; M7; and M1. In which, the biggest number of Grey relationship rankings in experiment 4 is 0.85. The highest level of Grey relationship level is considered to be optimized for technological parameters.

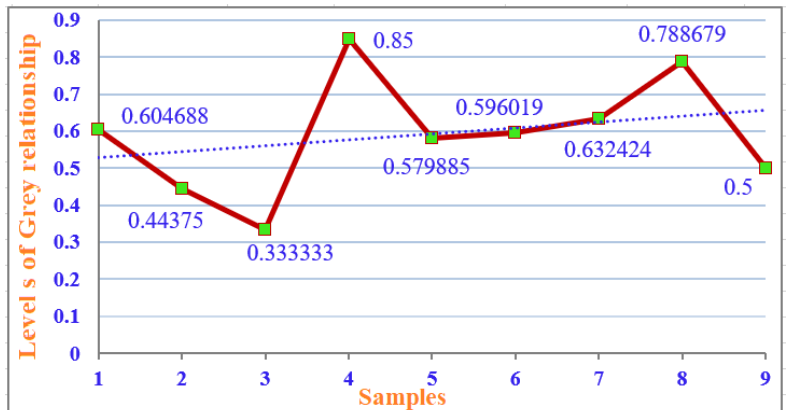


Figure 4.26. Grey correlation relationship

Combining the Grey and Taguchi relationships, determining the order of levels of technological parameters to the output parameters is the bonding strength of the welding layer with the substrate and

the weld hardness is the welding current intensity $I_{h2} = 7.5\text{kA}$, compression force of F1 electrode roller $F_1 = 1.7\text{kN}$; welding speed $V_{h1} = 1.5\text{cm/s}$, and the greatest effect is the welding current intensity with an impact percentage of 43,0%, followed by electrode compression force of 39,2%, finally welding speed of 17.8% is shown in Figure 4.27 and Figure 4.28.

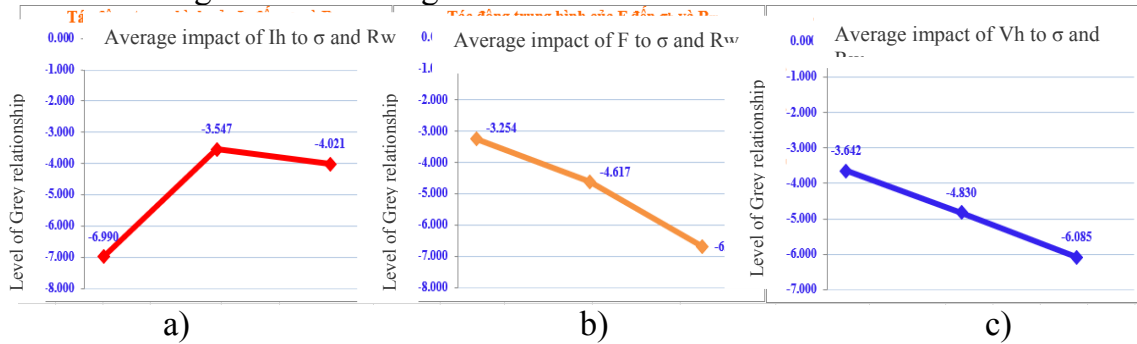


Figure 4.27. The classification chart of the influence level of I_h , F , V_h at the same time on the target of bonding strength to the substrate and weld hardness

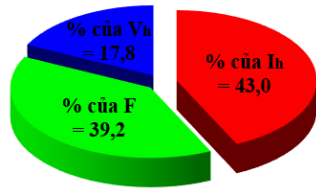


Figure 4.28. Chart of the influence percentage of I_h , F , V_h at the same time on the bonding strength to the substrate and weld hardness

+ From the results of calculating the Grey level in Table 4.7 using the application statistics software Minitab, can build a regression function showing the mathematical relationship of technological parameters with the two factors that are the bonding strength to the substrate and hardness of welding layer through Grey level as follows

$$Y_{dmt} = 0,194076.I_h^{1,25048}.F^{-1,27631}.V_h^{-0,992392}$$

The multi-objective optimization value based on the Grey level when replacing into the function of Y_{dmt} is:

$$\gamma_{i(opt)} = 0,819112$$

➤ According to the chart in Figure 4.27, the optimal level is I_{h2} , F_1 , V_{h1} , in which two parameters are compression force and welding speed at level 1. This value is in the boundary of the survey area, so to consider the relevance of the optional values in the boundary area, we search for the neighboring values of these levels based on the search algorithm by the double division method as follows:

The extended search level of neighboring optional elements is shown in Table 4.8

Table 4.8. The parameters at the same time affecting the bonding strength and weld hardness at a new level

Level	The affecting parameters		
	I_h (kA)	F (kN)	V_h (cm/s)
1	7.0	1.55	1.375
2	7.5	1.7	1.5
3	8.0	1.85	1.625

After 17 iteration of the searching rule according to the division algorithm, the optimal parameter set in the neighboring area with the desired optimal value of Grey level $\gamma_{i(opt)} = 0,819112$ is: $I_h = 7,81$ (kA), $F = 1,79$ (kN), $V_h = 1,47$ (cm/s). The optimal results when searching the neighboring area have a small deviation from the initial optimal value found by Taguchi method. The values of I_h and F are in the survey area, only V_h parameter is beyond the survey area but it has the deviation of 3% compared to the initial optimal level predicted by the Taguchi method.

The predicted results for the bonding strength of welding layer with the substrate, the hardness of the welding layer, the wear resistance of welding layer when considering the effect of simultaneous of three technological parameters are $\sigma_b = 460,8$ (N/mm²); $R_w = 54,7$ (HRC); $\Delta P = 0,0144$.

To assess the reliability of the optimal levels when considering the simultaneous effects of three parameters on the quality targets assessed through the verification results in Table 4.9, 4.10, 4.11, 4.12.

Table 4.9. The separation strength results of verification welding samples

No.	Sample name	Welding condition			Separation of pin			
		I_{h2} (kA)	F_1 (kN)	V_{h1} (cm/s)	Measurement (N/mm ²)			Average (N/mm ²)
					1	2	3	
1	Sample KC1	7,5	1,7	1,5	477	462	470	470

Table 4.10. The hardness results of verification welding samples

Rockwell Hardness measurement (HRC)										
No.	Sample name	I_{h3} (kA)	F_1 (kN)	V_{h1} (cm/s)	Measuring position					Average
					1	2	3	4	5	
1	Sample KC1	8,5	1,7	1,5	56	55	55	57	56	56

Table 4.11. The wear resistance results of verification welding samples

No.	Sample name	I_{h3} (kA)	F_1 (kN)	V_{h1} (cm/s)	ΔP (g)	R (mm)	S (mm)	N (N)	Im (g/N.mm)
1	KC3	8,5	1,7	1,5	0.0134	15	580272	20	1.15463E ⁻⁰⁹

Table 4.12. Verification results for simultaneous effects of technological parameters

Sample name	Single target	Technological parameters	Predicted results by Grey	Test results	% deviation
KC4	Tensile strength of welding layer and base metal	$I_h = 7,8$ (kA)	460,7 (N/mm ²)	459 (N/mm ²)	0,37%
	Hardness of welding layer	$F = 1,8$ (kN)	54,7 (HRC)	54 (HRC)	1.28%
	Wear resistance	$V_h = 1,5$	0,0144 (g)	0,0140 (g)	2.8%

Summary of chapter 4

1. Through the study of welding macrostructure, the microstructure of the adjacent area with the substrate metal with good bonding, always ensuring the bonding strength of welding layer with a high substrate of recovery welding parts (can reach $81 \div 95\%$ strength of base metal). The area of thermal influence is very narrow. The weld has a relatively high surface hardness of about ($47 \div 55$ HRC), which meets the requirements of working surfaces in most shafts. The restored welding samples were evaluated for wear resistance through comparison of wear samples of the shaft by seam welding to recover the C70 steel filler wire with wear samples of high frequency C45 steel shaft parts and hardness indicating the test piece of the welding sample has a wear resistance of about 1.44 times higher than that of the newly refining test piece.

2. After-welding repair parts only need mechanical processing to reach the size without any heat treatment or further treatment, so the parts are not deformed or peeled. The shaft details having high wear resistance and strength always ensure the bonding strength of the welding layer, the recovery part itself retains the internal plastic strength due to low heat effect.

3. Using Taguchi method and ANOVA analysis of variance has been identified:

- The appropriate levels of technological parameters for the object function of the bonding strength of welding layer with the substrate is the highest at: $I_{h2} = 7,5$ (kA), $F_1 = 1,7$ (kN), $V_{h1} = 1,5$ (cm/s), while that of surface hardness and wear resistance of the welding metal is the highest at $I_{h3} = 8,5$ (kA), $F_1 = 1,7$ (kN), $V_{h1} = 1,5$ (cm/s). Besides, the influence ratio of the above parameters on each welding mechanical property is also calculated specifically.

- Establishing a mathematical model to show the relationship between mechanical properties and technological parameters by linear regression and power functions, thereby assessing the trend of the technological parameters mechanical properties of welding layers through interpolation graphs for the two types of functions mentioned above.

4. Combining the correlation analysis of Grey with Taguchi experimental design and the double division algorithm have found the optimal technological parameters for the two parameters of the weld function is the bonding strength of welding layer with substrate and hardness of welding layer at levels $I_h = 7,81$ (kA), $F = 1,79$ (kN), $V_h = 1,47$ (cm/s). At the same time, determining the most effective percentage of welding parameters is I_h 43.0 (%), followed by F 39,2(%) and the lowest V_h 17.8 (%) to two mechanical properties above.

CONCLUSIONS OF THE THESIS

From the results of theoretical and experimental research of the thesis, some main conclusions are drawn as follows:

1. The working ability of recovery shaft parts is determined by three important using properties: bonding strength of the welding layer to the substrate metal, wear resistance and hardness of the welding layer. The first of the three properties is important for the part to be restored.

2. Welds formed at the plastic temperature, welding bond formation process occurs only at the contact surface, so the solubility of the base metal into the filler metal is low, the filler layer will have good purity so it has high and uniform average hardness, welding productivity is high, less deformed welding parts and it is easy to automate welding procedure. The process of forming welds in the solid phase, the relationship between the bonding strength of the welding metal and the substrate metal depends on the deformation of the metal wire.

3. Metal layer welded from C70 material on C45 steel substrate with the bonding strength between the welding layer and the high substrate can reach 95% of the tensile strength of the material of C45 recovery welding axis sample. The area of thermal influence is very narrow, the weld has a relatively high surface hardness of 55HRC. The recovery welding samples are evaluated for wear resistance by comparing the wear samples of the welding axis restored by C70 steel contact seam welding with the wear sample of the C45 high frequency anneal steel axis parts with the same hardness indicating that wear samples of welding samples have a wear resistance of about 1.44 times higher than that of new high-frequency annealing axis samples, this result is obtained by the wear resistance of the filler material as well as the welds being forged in welding procedure, making the density of particles more tight and better abrasion resistance.

4. Determine the appropriate levels, percentage of effects, regression form of technological parameters for the objective function of bonding strength of welding layer with the substrate, surface hardness and wear resistance of the welding metal are the highest responding: $I_{h2}, F_1, V_{h1}; I_{h3}, F_1, V_{h1}; I_{h3}, F_1, V_{h1}$, through Taguchi experimental design, ANOVA variance analysis, Minitab application statistics software, numerical calculation software and Matlab programming.

5. Analysis of Grey correlation relationship - Taguchi experimental design combined with double division algorithm to find neighboring solutions, found the optimal technological parameters for simultaneously 2 criteria of welding mechanical properties which are the bonding strength of the welding layer with the substrate and the hardness of the welding layer at: $I_h = 7.8(kA), F = 1.8(kN), V_h = 1.5(cm/s)$. At the same time, it is possible to determine the impact level of each welding technological parameter to two criteria of the bonding strength of the welding layer with the substrate and the highest hardness of the welding layer is the welding current intensity I_h 43,0(%), followed by the electrodes pressure F 39,2(%), the lowest is the welding speed V_h 17,8(%)

LIST OF PUBLISHCATIONS

1. Nguyen Minh Tan, Le Van Thoai, Hoang Van Chau, Dao Quang Ke, Le Thu Quy (2015). *Research Hardfacing Technology for Rotate items by Automatic Seam Welding with Alloy Steel Wire* . The 4th National Conference of Science and Technology on Mechanical Engineering, Division 1 - Machinery Manufacturing Engineering, pp 36-43, HCMC, November 6, 2015.
2. Le Van Thoai, Nguyen Minh Tan, Hoang Van Chau, Dao Quang Ke (2015), *Improving productivity and quality of welding structure by submerged arc welding with additional metal powder*, The 4th National Conference of Science and Technology on Mechanical Engineering, Division 1 - Machinery Manufacturing Engineering, pp 118-195, HCMC, November 6, 2015.
3. Nguyen Minh Tan, Le Van Thoai, Hoang Van Chau, Dao Quang Ke (2016). *Study on a hardfacing technology for restoration surface of steel shaft C45 by automatic seam welding with alloy wire 65G* . National Conference of Science and Technology on Mechanics - Motivation. Hanoi University of Science and Technology, Volume 1, pp.363-368, October 13, 2016.
4. Le Van Thoai, Nguyen Minh Tan, Hoang Van Chau (2016), *Impact Resistance of Weld Metal by SAW with Additional Metal Powder*. National Conference of Science and Technology on Mechanics - Motivation. Hanoi University of Science and Technology, Volume 1, p.327-331, October 13, 2016.
5. Ngo Thi Thao, Le Van Thoai, Nguyen Minh Tan, Bui Van Khoan (2016), *Using inverse method for predicting heat generated in friction welding*, National Conference of Science and Technology on Mechanics - Motivation. Hanoi University of Science and Technology, Volume 1, p.288-293, October 13, 2016.
6. Nguyen Minh Tan, Ngo Thi Thao, Le Van Thoai, Hoang Van Chau, Dao Quang Ke (2016), *Hardfacing Technology for Dimensional Restoration of Steel C45 by Automatic Seam Welding Using Alloy Steel Wire*, Science and Technology magazine - Vietnam Academy of Science and Technology, Code 33 - 44 Volume 54 - No. 5A.
7. Nguyen Minh Tan, Le Van Thoai, Hoang Van Chau, Dao Quang Ke (2018), *Optimizing Technological Parameters of Resistance Welding for Adherence Strength of Shaft Coating*, Vietnam Mechanical Journal, No. 10, pages 31-39, ISSN 0866-7056.
8. Nguyen Minh Tan, Le Van Thoai, Ngo Thi Thao (2018), “ *Study on structure and mechincal properties of weld for hardfacing by resistance seam welding*”, Journal of Science and Technology – Hung Yen University of Technology and Education, No. 20, December, 2018, ISSN 2354-0575.
9. Minh Tan Nguyen, Van Nhat Nguyen, Van Chau Hoang, Shyh-Chour Huang (2019), *"Optimizing resistance welding parameters on Ashesion strength of c45 steel shaft by using taguchi method"*, Journal of Physics: Conference Series, IOP publishing, MEIE28142.